RESOLUTION AND LINE SHAPE IN SCINTILLATION COUNTERS

by

P. S. TAKHAR

A THESIS SUBMITTED IN PARTIAL FULFILMENT OF
THE REQUIREMENTS FOR THE DEGREE OF
MASTER OF SCIENCE

in the Department of

PHYSICS

We accept this thesis as conforming to the
required standard

THE UNIVERSITY OF BRITISH COLUMBIA

In presenting this thesis in partial fulfilment of the requirements for an advanced degree at the University of British Columbia, I agree that the Library shall make it freely available for reference and study. I further agree that permission for extensive copying of this thesis for scholarly purposes may be granted by the Head of my Department or by his representatives. It is understood that copying or publication of this thesis for financial gain shall not be allowed without my written permission.

Department of Physics

The University of British Columbia,
Vancouver 8, Canada.

Date April 8, 1963

ABSTRACT

An experimental study has been made of a number of factors that determine the pulse height resolution of Scintillation Counters. A statistical model is developed from which an analytic expression for the ideal line shape is obtained. Excellent agreement is found with observations using an artificial light pulser.

An attempt to understand the noise spectra, exponential and non exponential under various conditions, has been made. A comparison is made between non crystalline organic scintillators and sodium iodide crystals of similar sizes. It is shown that for gamma-ray detection an important contribution to the line width originates with variations in the light collection efficiency from different regions of the scintillators.

ACKNOWLEDGEMENTS

The author wishes to express his thanks to Dr. J. R. Prescott for suggesting this research and for his advice and supervision in performing the experiments and also for his assistance in computation and analysing the data.

Thanks are also due to Dr. J. B. Warren for his interest in this work after Dr. Prescott left for the University of Alberta.

TABLE OF CONTENTS

Fig. No. ILLUSTRATIONS

CHAPTER 1

1. Introduction

Although the scintillation counter is of great value in gamma ray spectroscopy because of its high efficiency (see for example the review article by Mott and Sutton (1958) it suffers from rather poor energy resolution. In the past there has not been any clear understanding as to what factors (for example, with sodium iodide thallium activated scintillator) set a limit of about 6% resolution for the full width at half maximum with 0.662 mev gamma rays from a Cs - 137 source, nor of the way in which the resolution varies with gamma ray energy. Obviously a quantitative theoretical understanding of the minimum width which might be achieved with a given photomultiplier would be of considerable value in attempts to improve the performance of the scintillation counter. The aim of the present work was to achieve a better understanding of the factors that limit resolution in scintillation counters. In this work particular attention has been given to the role of the photomultiplier, since, other things being equal, this sets a basic limit to the resolution that can be achieved.

Good reviews of the previous work are to be found in the article of Mott and Sutton, and Wright (1954) and Breitenberger (1955) who give detailed discussions of the theory of resolution in scintillation counters.

Breitenberger (1955) described the light transfer in terms of a four stage cascade process and gave a statistical analysis of various causes of the line width of a scintillation counter, He described the light transfer as a four stage cascade consisting of (a) Generation of photons in the scintillator, (b) Collection of these photons in the photo cathode, (c) Photo electric conversion and (d) Collection of photo electrons into the first dynode of the photomultiplier. He pointed out that these four relations are mutually interdependent and there are intrinsic connections among these four processes.

According to Breitenberger, known causes of the line width in a scintillator counter are (i) varying transfer efficiency, (ii) voltage stabilization, (iii) inhomogeneous luminescence yield throughout in crystal, (iv) interaction of edge and scattering effects, (v) non proportional scintillation response and others. Breitenberger had also shown that square of line width versus reciprocal energy could be described by straight line having certain intercept and slope, where intercept depends upon "energy dependent" transfer variance and slope on energy dependent - variance.

Engelkemeir (1956) showed that light per kilovolt was not constant for different gamma ray energies. Nemilow et al (1959) at the Academy of Science in Moscow showed measured results on sodium iodide (Th), cesium iodide (Th) and potassium iodide (Th) which agreed with the results of Engelkemeir.

Bisi and Zappa (1958) extending Breitenberger's ideas showed that below 100 kilovolt the straight line condition does apply to reasonable spectrometers. However, for energy above several hundred kilovolts this is not true, i.e. transfer variance decreases. This accounts for bending over of the square of line width versus reciprocal energy curve at high energies where total absorbed events are composed of multiple compton and pair production events as well as photo-electric events.

Meyer and Murray (1960) gave a theory relating light-per-unit energy to the density of ionization along the particle track which provided understanding of nonproportional response. A computer program was developed by Zerby et al (1960) for evaluating the light per unit energy for electrons starting from gamma ray data, which established light per unit energy curve for electrons. This was then incorporated in a Monte-Carlo program for calculating the pulse height spectrum for gamma ray spectrum. This was helpful in comparing the experiment and theoretical gamma-ray curves.

Iredale (1961) pointed out that it is necessary to include the effect of delta rays as the scintillation light produced per unit energy loss (dl/dx) for an electron varies with the density of ionization over a wide range of energies. dl/dx increases with the increasing ionization density. Thus a further increase in the number of electrons sharing the gamma ray energy results in an increase in the light output; consequently, there will be a spread in the light output, depending upon the distribution in number and energy of electrons involved in absorption. According to Iredale, two important processes which lead to variations

are the number of Compton encounters of the primary gamma rays and the number of delta rays, i.e. the electrons capable of producing further ionization, produced in the slowing down of electrons which originally share the gamma ray energy.

The above effects require the use of more general expression for relative variance, for example, when light emission does not follow the poission model and the transfer probability varies from event to event, as in the case when scintillations occur in different regions of a large scintillator. The present work was aimed to investigate all these effects including the role of the photomultiplier in particular.

CHAPTER 2

2. Theory of Line Shape in Scintillator Counters

2.1 Statistical Models

Basically, resolution and line shape in scintillation counters are determined by the statistical frequency function of five separate processes:-

(a) Light production in the scintillator itself,

(b) Light collection at the photo-cathode,

(c) Production of electrons at the photo-cathode,

(d) Collection of photo electrons at the first dynode,

(e) Multiplication in the photomultiplier dynode structure.

Each of the distributions can be described by a frequency function $f(x)$ or by an associated generating function $G(\theta)$, moment generating function $M(\theta)$ or characteristic function $x(\theta)$, defined as follows with the introduction of the auxiliary variable:

$$G(\theta) = \sum_{\text{all } x} \theta^{x} f(x)$$

$$M(\theta) = \sum_{\text{all } x} e^{\theta x} f(x)$$

$$x(\theta) = \sum_{\text{all } x} e^{i\theta x} f(x)$$

or by corresponding integral of the frequency function if continuous. The moment generating function is obtained from the generating function by replacing $\log \theta$ by $i\theta$ and the characteristic function by replacing $\log \theta$ by $i\theta$ and vice versa. The moments of the frequency function are found as

functions of the derivatives of $G(\theta)$, $M(\theta)$ or $x(\theta)$ evaluated at $\theta = 1$ in the case of generating function or $\theta = 0$ in the case of $M(\theta)$. For example, the first moment, μ, about the origin (the mean) of $f(x)$ is given by $\mu = M(0)$ and variance, σ^2 (second moment about the mean) by: $\sigma^2 = M''(0) - M'(0)^2$ Primes denote differentiation with respect to x. The characteristic function is the Fourier transform of the frequency function which can therefore be found (at least in principle) once the characteristic function is known. Since the statistical processes listed above are in cascade, the following property of the generating function can be used to find the generating function of the outcome of the cascade: let $X(\theta)$, $Y(\theta)$, $Z(\theta)$ represent the generating functions of three processes in cascade, then the generating function $G(\theta)$ of the output frequency function is given by the functional:

$$G(\theta) = X\left\{Y\left\{Z(\theta)\right\}\right\}$$

If U_x, U_y, U_z, represent the means of the frequency functions $f(x)$, $f(y)$, $f(z)$ then $U_G = Ux\ Uy\ Uz$. Introducing the dimensionless relative variance V = Variance/ $(\text{mean})^2$, i.e.

$$V = \frac{\sigma^2}{\mu^2} \quad \text{then} \quad V_G = Vx + \frac{Vy}{Ux} + \frac{Vz}{UxUy} \qquad (1)$$

The extension to a cascade of more than three processes is evident.

For the purposes of comparison with experiment statistical models must be sought for the five processes listed above. In the present work the following models have been adopted:

(a) Light production: an average of n primary photons, having a Poisson distribution, for which the generating function is $\exp(n(\theta - 1))$. (See Appendix). This model is plausible so long as we assume that the events in which photons are produced are independent. In any case, Breitenberger

shows, that regardless of the precise form of the frequency function for which $\bar{n}$ is the mean, it becomes effectively Poissonian provided a sufficiently small fraction of photons is allowed to reach the photomultiplier; this was so in the present experiments and the model appears to be justified by experimental results.

(b) (c) (d) Light collection, photo-electron production and collection:

In so far as each of these processes constitutes a Bernoulli trial, e.g. a photo electron released from the cathode either reaches the first dynode or it does not, each can be represented by a binomial distribution having the generating functions $P(\Theta) = 1 - p + p\Theta$ where P is the probability of a "successful" event, e.g. a photo electron reaches the cathode. Since any number of binomial processes in cascade generates a binomial frequency function (see Appendix), all three processes can be taken together into a single generating function $T(\Theta) = (1 - \gamma) - \gamma$, where γ is the probability that a primary photon will result in an electron arriving at the first dynode. It is conveniently referred to as the "transfer probability". Strictly speaking, of course, the arrival of an electron at the cathode does not guarantee that a cascade will reach the anode of the photomultiplier. A cascade may fail to start, or once started, it may "break" at the subsequent dynode. Although this is technically part of the multiplication process, it may be shown (see Appendix) to be formally equivalent to a reduction in the number of electrons reaching the first dynode, i.e. to a reduction in γ.

At this stage of the argument, non uniformity of the photo cathode

is irrelevant since the only requirement is that τ should remain constant from event to event. This is shown formally by Breitenberger and confirmed by the observations of Hickock and Draper (1958) in their Fig. 17 and in the present experiments.

The above property of binomial distributions in cascade to generate another binomial distribution allows one artificially to vary the transfer efficiency by means of filters interposed between the light source and photo cathode, as described in later sections.

The generating function for a cascade consisting of a Poisson distribution followed by a binomial distribution is again Poissonian (see Appendix) viz. exp. $(n(\theta - 1))$ in the above notation having a mean $n\tau$.

(e) Multiplication: The multiplier structure is a complex system itself involving a cascade of processes in which a single electron falling on the first dynode produces a distribution in the number of electrons arriving at the anode, and hence in the voltage pulse observed there.

If we make no assumptions at this stage about the model to be used for the dynode statistics, then on the basis of a three-stage chain consisting of Poisson light production, binomial transfer, and multiplication on an arbitrary model, with relative variance Vm, relation (1) takes the very simple form: (see Appendix)

$$V_G = (1 + Vm)/n\tau \qquad (2)$$

Thus, regardless of the details of the statistical model used in

describing the multiplication, the relative variance, V_G of pulses at the output of photomultiplier, is inversely proportional to n, the number of electrons arriving at the first dynode.

It should be noted that the particularly simple form of relation (2) is a consequence of the choice of a Poisson distribution for the model of light production and that it is only true if τ is constant for all events considered. Breitenberger shows that if τ itself varies from event to event, as is certainly the case when scintillations occur in different regions of a large scintillator, then expression (2) must be modified to read: (See Appendix)

$$V_G = V_T + (1 + Vm)/n\tau \qquad (3a)$$

where V_T is introduced by the non constancy of τ and the graph of V_G versus $1/n\tau$ is linear with a positive intercept V_T on the V_G axis. A similar result is obtained if instrumental resolution is disproportionately large. If, in addition $\underline{n}$ is not from a Poisson distribution but one which has a relative variance Vn, then expression (3a) becomes:

$$V_G = V_T + (1 + V_T)\left(Vn - \frac{1}{n}\right) + \frac{1 + Vm}{n} \qquad (3b)$$

This reduces to:

$$V_G = \left(Vm - \frac{1}{n}\right) + \frac{1 + Vm}{n} \qquad (3c)$$

if there is no variation in τ from event to event.

The effect of variability in τ or $\underline{n}$ which gives rise to the latter result should be clearly distinguished from the case where τ or $\underline{n}$ is varied deliberately in order to vary the observed pulse height. Since expression (2) is symmetric for $\underline{n}$ and τ, either or both may be varied

for this purpose and provided that both then remain constant, expression (2) still correctly describes the variability of the pulses observed. In expression (3), however, such variation in τ may also likely effect V_T.

2.2 The shape of the ideal scintillation line

If we now choose an explicit mathematical model for the distribution of single electron pulses in the multiplier, we can, at least, in principle, determine the shape of the ideal scintillation line.

The fact that the single-electron distribution is nearly exponential, which appears from the experimental results in the later part of Chapter 3, suggest choosing a simple exponential as a model. We therefore take for the frequency function of single-electron pulses $G(X) = a^{-1} \exp(-X/a)$, where X is any convenient measure of pulse height. The generating function for this frequency function is $1/(1 - a \log \theta)$ (see Appendix) and the generating function for a cascade consisting of Poisson light production, binomial electron collection and exponential multiplication is:

$$G(\theta) = G_1 (G_2(G_3(\theta)))$$

Where G_1, G_2 and G_3 represent the generating functions of Poisson, binomial and exponential distributions and are given by

$$G_1 = \exp(n(\theta - 1))$$

$$G_2 = \left\{\tau\theta + (1 - \tau)\right\}$$

$$G_3 = \frac{1}{1 - a \log}$$

Therefore, for the cascade of three

$$G(\theta) = \exp\left\{n\left(\frac{}{1 - a \log \theta} - (1 - \tau)\right) - 1\right\}$$

or

$$= \exp \frac{n a \tau \log \theta}{1 - a \log \theta} \quad \text{(see Appendix)}$$

Replacing $\log \theta$ by $i\theta$ gives characteristic function:

$$\chi(\theta) = e^{-n} \exp\left(\frac{n\tau}{1 - ia\theta}\right)$$

which is the Fourier transform of the required frequency function $f(x)$

$$f(x) = \frac{1}{2\pi} \int_{-\infty}^{+\infty} e^{-i\theta x} \chi(\theta)\, d\theta$$

The regular solution (Campbell and Foster 1960) is:

$$f(x) = N^{\frac{1}{2}} a^{-\frac{1}{2}} e^{-N} X^{-\frac{1}{2}} \exp(-X/a)\, I_1 \left\{ 2(NX/a)^{\frac{1}{2}} \right\} \qquad (4)$$

Where I_1 is a modified Bessel function of the first kind for imaginary argument, and N replaces $n\tau$, the mean number of electrons reaching the first dynode.

The solution also includes a delta function of the magnitude e^{-N} at the origin, which is evident by pattern N = 0 in the Poisson distribution which describes the first two stages, representing the cascades that break or fail to start. The properties of the distribution are as follows: (see Appendix)

$$\text{Mean } \mu = Na$$

$$\text{Variance } \sigma^2 = 2Na^2$$

hence relative variance $Vx = 2aN^{-1}$

Third moment about the mean $6a^3N$

It has a finite value at X = 0 and is a model for $n \leqslant 2$. It is skewed to the left i.e., the mode occurs at lower values of x than does the mean. For large N the mode tends to (N - 2)a (Appendix) and the distribution as a whole tends to Gaussian. There is a particularly

simple relationship between the variance and the mean viz $\sigma^2 = 2\alpha\mu$ i.e., the variance is proportional to the mean and constant of proportionality is twice the logarithmic decrement of the exponential. For sufficiently large values of the argument of the Bessel function $(2(NK/a)^{\frac{1}{2}} > 10$ the asymptotic form for the latter is substituted and the frequency function becomes:

$$f(X) = (4\pi)^{-\frac{1}{2}} N^{\frac{1}{4}} (X/a)^{\frac{3}{4}} \exp\left(2(NX/a)^{\frac{1}{2}} - x/a - N\right) \qquad (5)$$

2.3 Statistical factors in the Scintillators

In addition to the photomultiplier effects discussed above, the scintillator itself introduces additional sources of statistical fluctuations. The most obvious stems from the fact that the scintillator occupies a finite volume. For purely geometrical reasons, scintillation events taking place in different regions of the scintillator result in different numbers of primary photons reaching the cathode, so that the frequency function of the transfer is no longer binomial when averaged over a number of events. An explicit calculation of this geometrical effect has been carried out by Kukushkin and Ratner (1958) for a sodium iodide crystal and Hickock and Draper (1958) have estimated it for sodium iodide from measuring made with a variety of crystals and photomultipliers. Similar analyses have been made by Burch (1961), Barnaby and Barton (1960), and Brini et al (1955). Other contributions to variance are flaws and inhomogeneities in the crystal as given by Wright (1954) and Garlick and Wright (1952), edge effects, and the possibility that the fluorescence mechanism in the scintillator is not Poissonian. Kelley et al Breitenberger (1955) (1956) have suggested that sodium iodide has an "intrinsic resolution" that is characteristic of the material regardless of its geometrical form. Wright and Garlick (1954) drew similar

conclusions for crystals of calcium tungstate, potassium iodide and diamond. Bisi and Zappa (1958) discuss the role played in resolution by the multiple interactions that characteristically contribute to the full-energy peak for gamma-ray detection in sodium iodide and Zerby, Meyer and Murray (1961) and Iredale (1961) have elegantly demonstrated that such multiple interactions combined with non-proportional energy response, Murray and Meyer (1961), result in an "intrinsic broadening" of gamma-ray lines which is significant contribution to the total line width. Burch (1961), and Iredale (1961) have discussed fluctuations in the number of delta-rays along an ionising track as a further source of line width.

The above effects require the use of the more general expressions (3a), (3b) and (3c) of Chapter Two for the relative variance V_G of the scintillation line. It will be recalled that if the light emission does not follow the Poisson model, then

$$V_G = (Vn^{-1}/n) + (1 + Vm)/n\tau \qquad (6)$$

Where V_n is the relative variance for the production of photons; and if in addition the transfer probability varies from event to event, as in the case when scintillations occur in different regions of a large scintillator, we then have:

$$V_G = V_T - (1 - V_T)\ (Vn^{-1/n}) - (1 + V_m)/n\tau \qquad (7)$$

where V_T is basically the relative variance of the frequency distribution of transfer probabilities. In a practical scintillator V_T may also include, additively, effects intrinsic to the scintillator (Terby and Meyer (1961) and Iredale (1961)) and be energy dependent. The last term in each of these expressions represents the contribution of the photomultiplier to V_G.

In Section 4.6 and the following sections an attempt has been made to account for the effect of variable transfer probability on resolution, and we shall refer to this contribution to V_T as the "transfer variance".

2.4 The Addition of Random tube noises

At room temperature, spontaneous emission of electrons from the cathode may modify the above distributions. A fraction, P of the light signals will have the above frequency function but the remaining fraction (1 - P) will be accompanied by one or more electrons independently (and randomly) emitted from the photo cathode. Under normal conditions the fraction (1 - P) is small enough to make the probability of simultaneous emission of more than one electron negligible, and we consider only the two alternatives of zero or one random electron accompanying the light signal. Since these two alternatives are mutually exclusive, the final frequency function is the appropriately weighted sum of the frequency functions appropriate to zero and one extra electron respectively. The former has already been found above in expression (6). The latter is found as follows:

Since the random emission and the light signal are independent, the generating function of their sum is found as the product of the individual generating functions, viz:

$$\frac{\bar{e}^N}{1 - a \log \theta} \quad \exp \left(\frac{N}{1 - a \log \theta} \right)$$

from which the frequency function F(x) is found as before via the characteristic function, to be

$$f + 1 \quad (x) = a^{-1} e^{-N} e^{-X/a} \quad I_o \quad (2(NX/a))^{\frac{1}{2}} \qquad (8)$$

Where I_o is so modified Bessel function of the first kind and the remaining symbols have their former meanings. The mean is $(N - 1)a$ and variance $(2N - 1)a^2$; for large N the mode tends to N a and distribution as a whole to normal. Combining the two distributions (4) and (6) gives:

$$F(X) = Pf(X) + (1 - p) f + 1(X)$$

$$\mu_F = (N - 1 - P)a$$

$$\sigma_F^2 = (2N - 1 - p^2)a^2$$

Except for small N (say less than 4) the distribution f(X) and f(+)1(X) are so similar in shape that a small admixture of one with the other does not produce much change in the shape of the distribution. In particular, the ratio σ_F/μ_F is quite insensitive to the value of P and for all practical purposes it can be taken as equal to 2a. The later fact was confirmed by observation at room temperature but no frequency functions were computed. Because of the similarity of the expressions (4) and (8) no corrections were made to the distributions taken at any dry ice temperature.

CHAPTER 3

Experimental Technique

3.1 Scintillators used

(1) Liquid Scintillator:

The liquid scintillator used in the present study was NE-219 supplied by Nuclear Enterprises, Winnipeg. This highly purified monoisopropylbiphenyl employed in NE-219 is relatively free from oxygen-quenching effects normally encountered in liquid scintillators. This is a liquid scintillator of low volatility and low toxicity and no special sample preparation is required.

This gives about 55% of the pulse height from an Anthrecene crystal phosphur under similar circumstances and has the wave length of maximum emission of 4300 A.U. The monoisopropylbiphenyl based liquid scintillator gives counting efficiencies of 83%, 78% and 31.5%, for I^{131}, P^{32} and C^{14} beta radiation respectively.

Liquid scintillators were contained in glass cells and were stored in clean dry sealed containers in the dark.

(2) Plastic Scintillator:

Plastic scintillators were used in the present work for alpha-radiation and as well for gamma-radiation and were NE-102 of $1\frac{1}{2}$ inches diameter and of various thicknesses.

NaI MOUNT FOR ALPHA RAYS

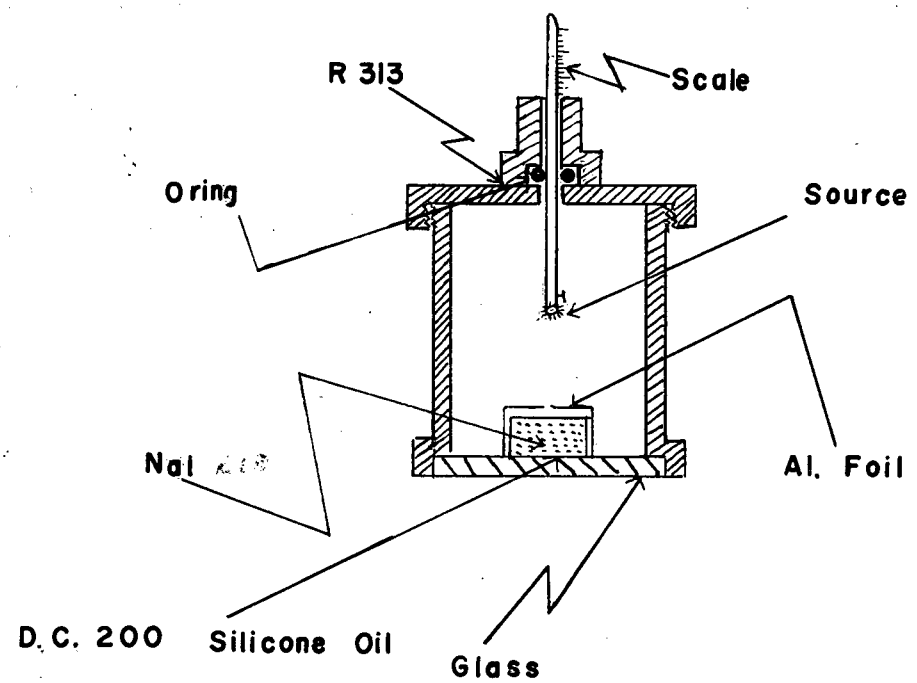

Fig. I

(3) Inorganic Scintillators:

The inorganic scintillators used were sodium iodide activated cylindrical crystals of 1, 1½, and 2 inches in size, obtained from Harshaw Chemical Co. These were used for the study of resolution. For comparison with the organic scintillator mainly the 1 inch size was used. A two-inch crystal was cut in the steps of .5, 1.0, 1.5, 2.0, 2.5, 3.0, 5.0 cms. to study the resolution with different crystal sizes. Also one thin strip was prepared for the study of resolution in NaI (Th) with alpha-particles.

3.2 Assembling technique for Scintillators:

(1) Liquid Scintillator Assembly:

The liquid scintillator assembly used for NE-219 is shown in Fig. 1. A container of the size 1½ inches diameter and 1 inch depth was made out of pyrex. For the reflector it was covered with a thin sheet of aluminium along the inside wall and a circular disc of aluminium with 1/8 inch hole in the centre for the Alpha source was used at the top. These discs were always prepared specially according to the depth of the liquid scintillator. The container was filled with liquid 1¼ inch deep or less, depending upon the requirements, and was coupled to the photomultiplier with D.C. 200 silicone oil.

(2) Plastic Scintillator Mounting:

The plastic scintillator NE-102 was coupled to the photomultiplier with D.C. 200 silicone oil. At the top and along the sides it was covered with a thin sheet of aluminium with a hole of 1/8 inch in the centre of the top for an alpha source. For gamma radiation the

NaI MOUNT FOR GAMMA-RAYS

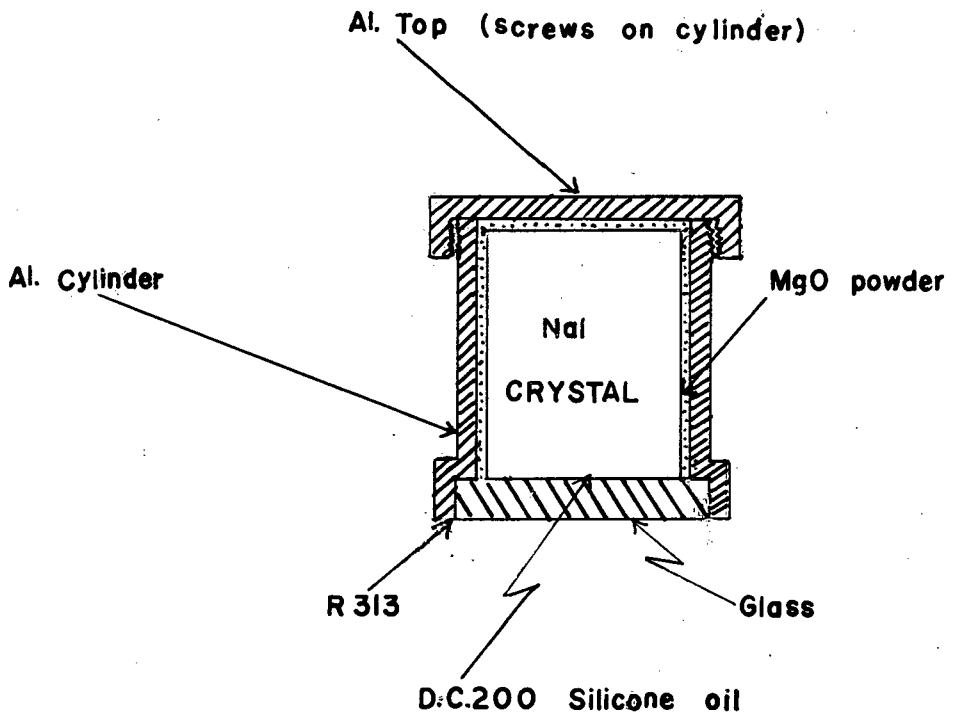

Fig. 2

plastic crystal was mounted in an aluminium container with magnesium oxide as a packing medium for the reflector.

(3) Sodium Iodide mounting technique:

Since the sodium iodide crystals are deliquescent, any arrangement for mounting the crystal must provide perfect protection against water vapour present in the air. R. K. Swank (1952) has reported a method of mounting crystals using the highly efficient, diffuse reflecting properties of powdered magnesium oxide. This technique requires dry mounting of the crystal even free from the mineral oil in which they are stored, since the reflecting properties of the magnesium are destroyed if oil is present. For these reasons sodium iodide crystals were mounted in a "dry box" in which there were arrangements for removing the moisture from the atmosphere by circulation of the air present over a drying agent such as phosphorous-pentoxide.

To start with, the crystal is rough polished outside the dry box. This is carried out by using emery powder and mineral oil. The crystal is then transferred to the dry-box, wiped free of oil and then ground through successively finer grades of abrasive until a high polish is achieved. It is then mounted in a sealed aluminium container with a 1/32 inch pyrex window and removed from the dry box and attached to the photomultiplier using bleached vaseline as optical coupling. A typical mount for NaI crystals is shown in Fig. 2. For the sodium iodide strip used for studying the resolution in the case of Alpha radiation, the mount is shown in Fig. 3.

LIQUID SCINTILLATOR NE 219 ASSEMBLY.

HALF SCALE

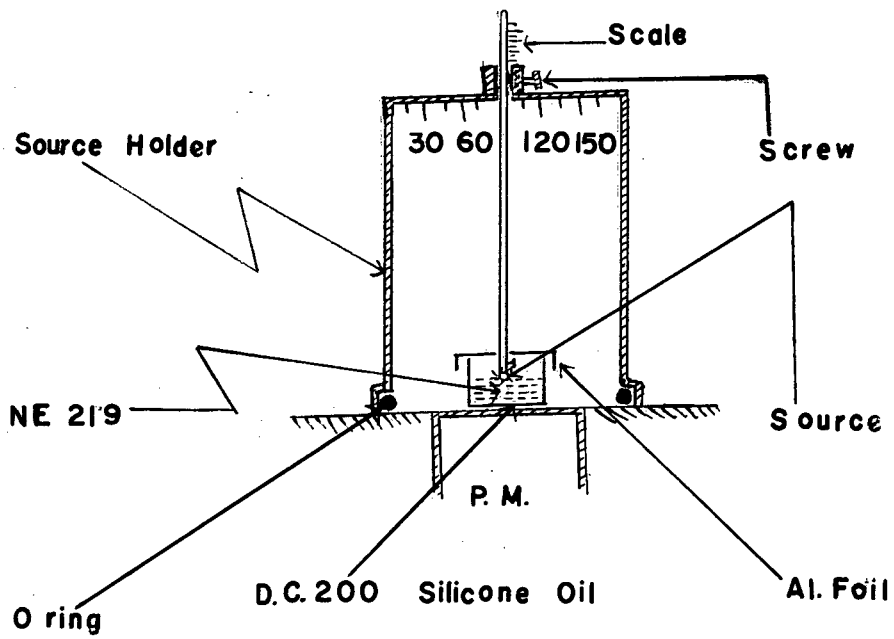

Fig. 3

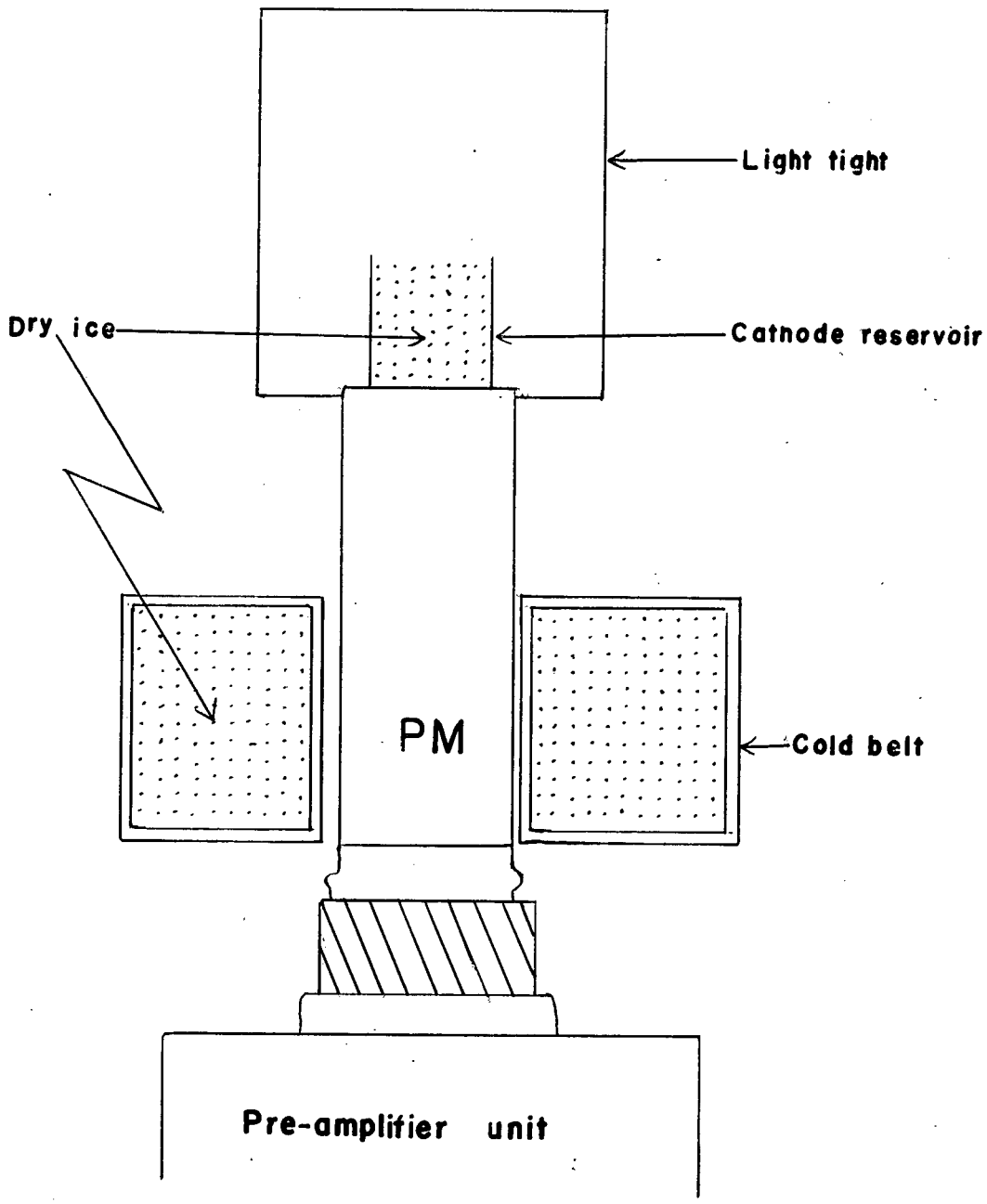

COOLING ARRANGEMENT FOR PHOTOMULTIPLIER

Fig. 4

In addition to the above technique the following conditions must be met while mounting the sodium iodide crystals:

(a) The mount must be air-tight as well as light-tight so that no moist air can go in.

(b) The optical coupling to the photo cathode of the photo-multiplier must be good taking care that no air bubble is present in between.

(c) The fluorescent light must be extracted with a uniform high efficiency from all parts of the crystal.

(d) The X-Rays must enter the crystal with little absorption and scattering.

(e) Aluminium foil with a 1/8 inch hole on the top of the NaI strip was used in the case of Alpha-particles, instead of MgO reflecting powder.

3.3 Arrangement for cooling the photomultiplier

The method used for cooling the 6810A photomultiplier, for which the noise spectrum at dry ice temperature has been studied, is shown in Fig. 4.

For the cooling of the photo-cathode a simple barrel made out of Bristol board of about two inches diameter filled with powdered dry ice was used. The noise spectrum was taken as the photo-cathode was cooling down.

For the cooling of the photomultiplier itself a similar belt surrounding the photomultiplier body filled with dry ice was used and the noise spectrum was again taken as described in Chapter 4.

SOURCE HOLDER

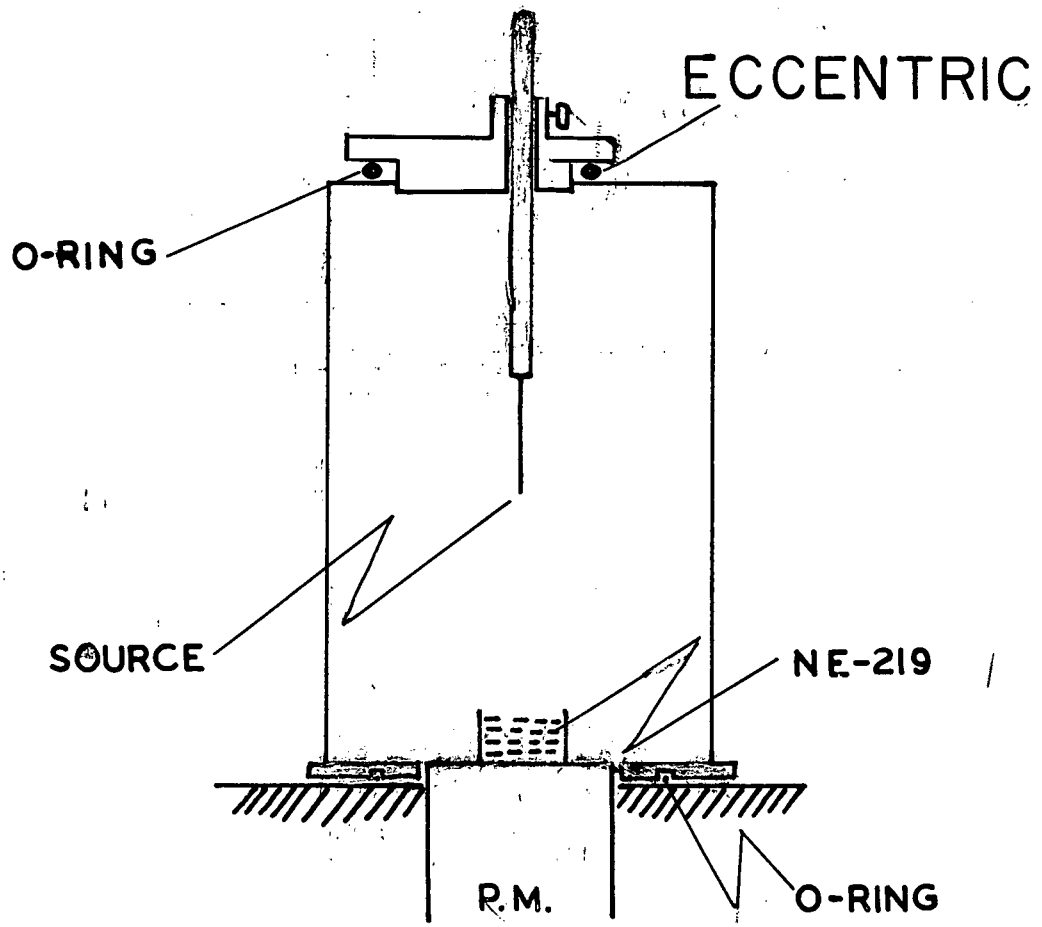

Fig. 5

3.4 Alpha Source Holder for source position adjustment with the liquid scintillator

The checking of the uniformity of NE-219 was achieved by designing an alpha-particle source holder as shown in Fig. 5 so that the source can be moved in any position in the liquid scintillator by means of two eccentric rotating seals. The whole body of the holder rotates and the source can be placed at any radial distance by rotation of the upper seal. This arrangement was used for scanning the photo-cathode. Also the distance of the course from the photo-multiplier can be varied by moving the rod carrying the source.

3.5 Radiation Sources

(1) Alpha Emitters:

The alpha particle source consisted of Po^{210} deposited on a plane polished silver foil of 1/8 inch diameter from the solution of Polonium in 0.5N hydrochloric acid. This thin foil was attached to one end of a glass rod of about the same diameter and about 3 inches long. The glass rod could be mounted on the source holder rod. This source of 5.3 Mev alphas has negligibly small thicknesses as measured on the British Columbia magnetic analyser by Mr. S. Smith.

For the study of transfer effects within the liquid scintillator NE-219 a small alpha particle source was made by depositing Po^{210} on the end of length of silver wire 0.030 inches in diameter for a distance of about 1 m.m.

(2) Gamma Sources:

Gamma Sources used were Co^{57}, Hg^{203}, Cs^{137}, Na^{22}, Co^{60}, Zn^{65}

LIGHT PULSER

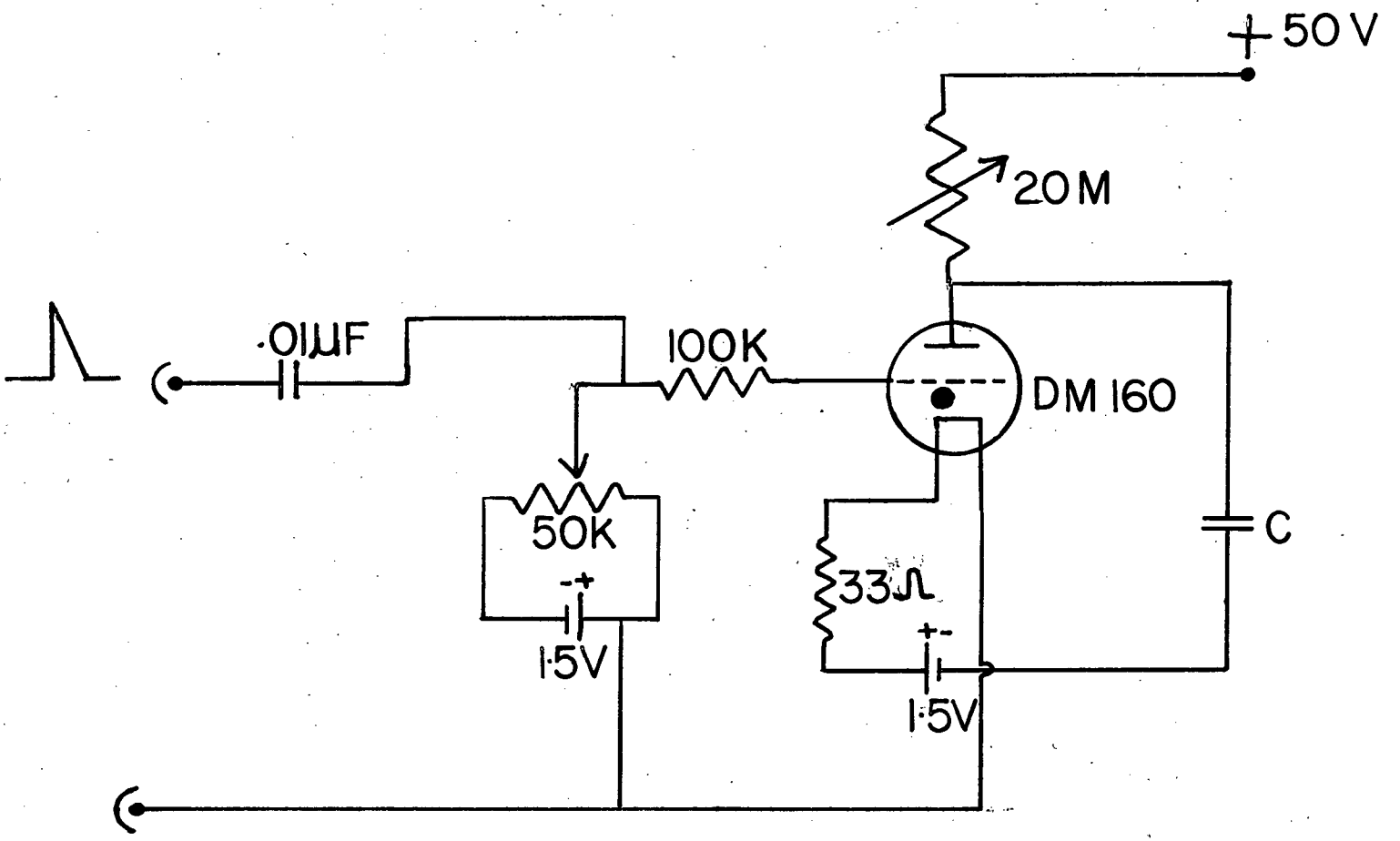

Fig. 6

and $RaTh^{232}$ with energies .123; .273; .662; .51 and 1.28; 1.17; 1.33; .511 and 2.62 MeV respectively.

(3) Light Sources:

Pulsed light signals were initially provided by a neon lamp pulser of the type described by Hickock and Draper (1958) and by Garlick and Wright (1952) but this proved rather unreliable and a pulser using Phillips DM 160 (6977) - (Prescott and Linquist (1961)) was developed.

The DM 160 is a voltage indicator tube. It is a directly heated subminiature tube and it has a phosphor coated anode (Jedec, P-15) which is dark when the tube is biased beyond the grid bias but which glows green for negative bias less than about 3V under the recommended operation conditions, i.e. plate voltage 50V, filament voltage 1.5 as shown in Fig. 6. The intensity of light output is a function of grid voltage and may readily be varied by changing the same. Normally in operation the tube is biased beyond cut-off and pulsed on by means of positive pulses of arbitrary shape of rise time 0.05 μ sec applied to the grid. The measured rise time at the cathode of the photomultiplier was about 1 μ sec. The flasher continued to operate satisfactorily (though with reduced light output) with square grid pulses even as narrow as 0.1 μ sec. Viewed end on at a distance of 25 cm. and with grid pulses 2 μ sec. wide the output pulse height was variable and stable, over a range of pulses barely distinguishable from tube noise to pulses equivalent of a one MeV electron in NaI (Th). Larger pulses can be obtained by increasing the plate voltage. Over a period of hours the flasher was at least as stable as the associated Photomultiplier assembly.

BLOCK-DIAGRAM OF ELECTRONICS.

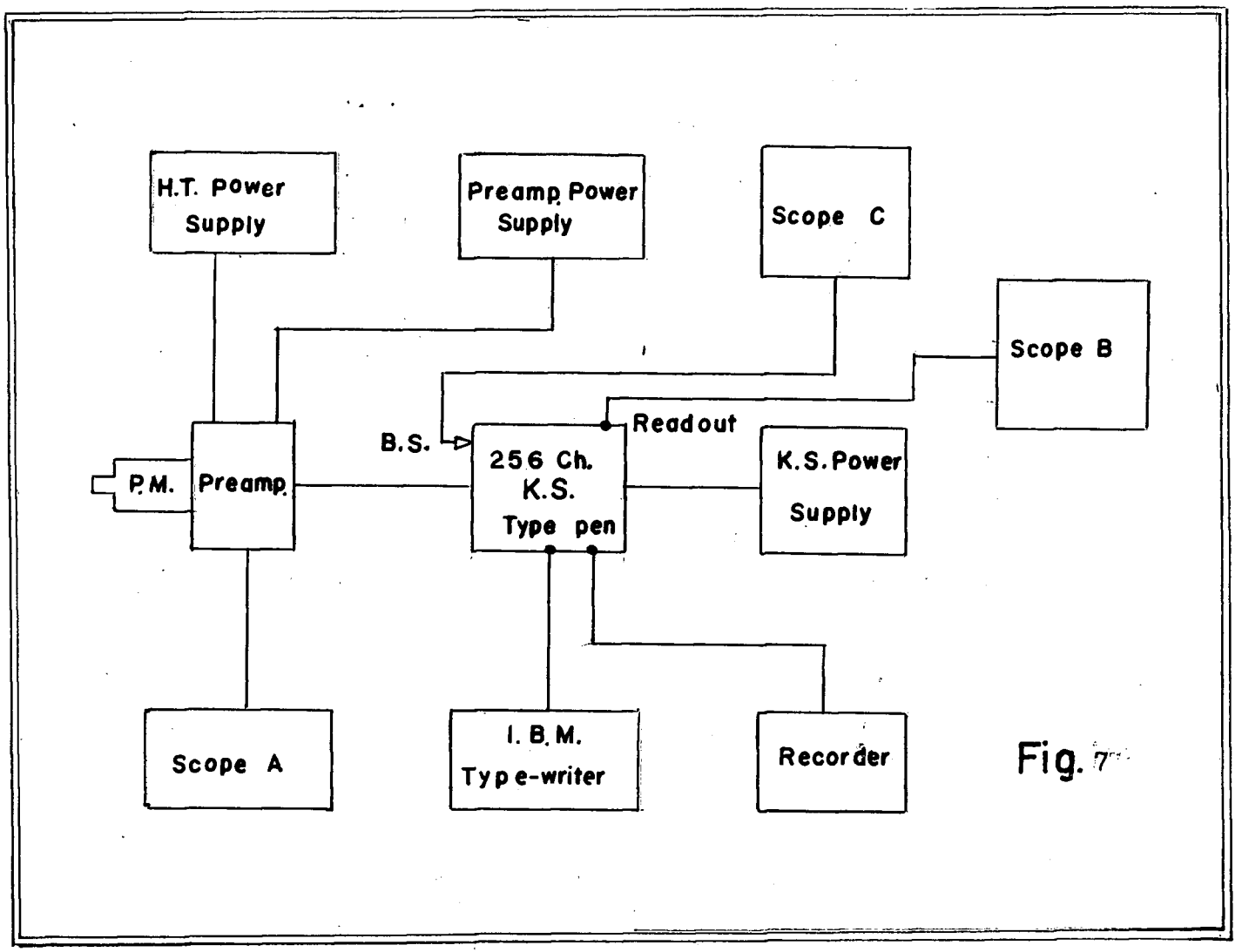

Fig. 7

In the end-on viewing position light from the filament produced no measurable increase in Photomultiplier noise and in any case may be reduced either by use of an optical filter or by under-running the filament, which operates satisfactorily at currents as low as one third of rated heater current.

3.6 Electronics and data recording

A block diagram of the electric i.e. apparatus is shown in Fig. 7 with this experiment designed to investigate, the following factors were carried out:

(I) Noise and multiplier statistics

(II) Noise and resolution

(III) Experiment verification of the shape of the ideal scintillation line

(IV) Non-exponential single electron distribution

(V) Transfer effects in organic scintillators

(VI) Transfer effects in a sodium iodide scintillator

(I) Photomultipliers

The photomultipliers used in this study were RCA types 6342, 6810, 6810A and 7046, the latter one being a 5" tube. In preliminary studies, the behaviour of the first three types was found to be very similar and results are reported here only for 6810A and 7046. Both of these tubes offer independent control of the focussing conditions. In the case of the 7046 two such controls are provided. The setting of the control designated "Grid" was found to have insignificant effects for the purposes of the present investigation and was usually left in

mid range. The distribution of voltages on the various dynodes was that recommended by the manufacturer for low light level applications. Signals on the anode of the photomultiplier were differentiated with a time constant of 40 μ sec. and analysed in a Nuclear Data ND101 256 channel Kick-sorter as described later.

(II) H. T. Power Supply

The regulated high voltage model RE5001 AWI of North East Scientific Corporation, Cambridge, Mass., was used to maintain the highest stability. Since the gain of the photomultiplier is very sensitive to the voltage applied, a supply of exceptional long term stability is required. The above model gives reasonable results.

(III) Preamplifier Power Supply

This unit is also a commercial regulated power supply, Model 25, made by Lambda Electric Corporation, College Point, New York, which was fairly stable throughout the work.

(IV) Oscilloscope A, B and C

A was a Model 513 - A "Tekronix" oscilloscope. It was used for the investigation of pulse shape and sizes at various points. No quantitative measurements were made with it except for scanning of the photomultiplier with the light pulser. Mostly it was just for setting up the apparatus.

Oscilloscopes B and C were of the type of RM 31 A supplied by Tekronix Inc. The scope B was used for displaying the spectrum from

the memory of ND 101 before the final print out and the scope C was connected to the "Busy signal" which shows the output pulse from the Kicksorter amplifier while it is analysing.

(V) ND 101 256 Channel Kicksorter

The ND 101 is a commercially built unit supplied by Nuclear Data Inc. The analyser is capable of handling pulses at the rate of 30,000 per sec. with maximum pulse size .3 volts and 30 - 40 μsec. long. A check was made with various frequencies of pulses, 2 K.C. - 30 K.C. and with various lengths of pulses before it was used in the present studies. Also certain results in the present studies were checked by a 100 channel Kicksorter in our laboratory.

The incoming pulse after amplification charges a condenser, this pulse stays flat for .2 μsec. then the condenser is discharged with constant current. The oscillator starts as soon as the voltage on the condenser reaches maximum and continues oscillating until the capacity is discharged. The number of oscillations depends on pulse height, these are then counted and fed to the memory in the proper channel depending upon pulse height.

The whole spectrum can be displayed on an oscilloscope when in "Read Out" position. then it can either be printed or penned, i.e. plotted according to the requirement. Gain settings were calibrated with a standard pulser and the relative gain as well as zero was found.

The special arrangement used for the study of low level pulses is shown in Fig. 10.

CATHODE FOLLOWER

FOR USE WITH 7046 PHOTOMULTIPLIER.

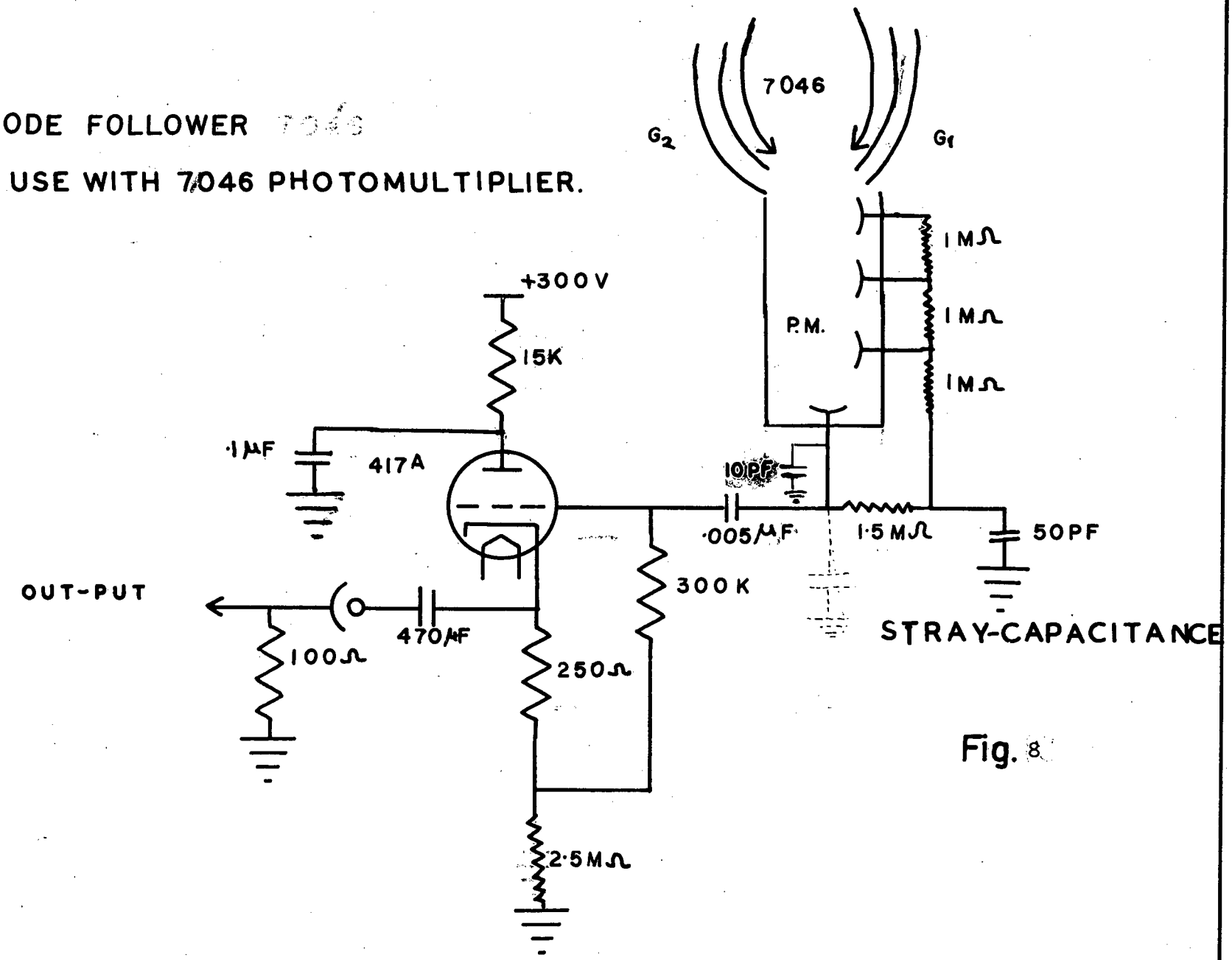

Fig. 8

(VI) Preamplifiers for 7046 and 6810A Photomultipliers

For the 7046 photomultiplier a preamplifier with gain of unity using 417A tube was used to feed a 100 ohm line transmitting the pulses from the photomultiplier. No amplifier stage was included, since it was felt that pulses available from photomultiplier tube were sufficiently large for analysing purposes as the amplifier of the ND 101 requires only .3 volt pulses. The preamplifier for the 7046 photomultiplier is shown in Fig. 8.

A white cathode follower used for the 6810A with a 6BQ7A tube is shown in the Fig. 9. This was also designed with gain of unity. A white cathode follower is suitable for both negative and positive pulses and it will develop undistorted signals across a substantial stray capacity as with a positive going wave front the upper half of 6BQ7A can conduct strongly to change the stray capacity while on negative going wave fronts the capacity is discharged by a heavy current in lower part of the 6BQ7A.

The action of a simple cathode follower is to maintain a constant potential difference between the grid and the cathode. Similarly in this case if, for example, the cathode or output voltage should be too negative the upper half will pass more current developing a negative signal at its anode which causes the lower half to pass less current. The changes in both the parts tend to restore the cathode potential to its correct value. In the quiescent state with no input signal the cathode voltage of the upper half adjusts itself so that current in the upper part is the same as specified by the bias conditions in the

CATHODE FOLLOWER FOR USE WITH 6810 A PHOTOMULTIPLIER

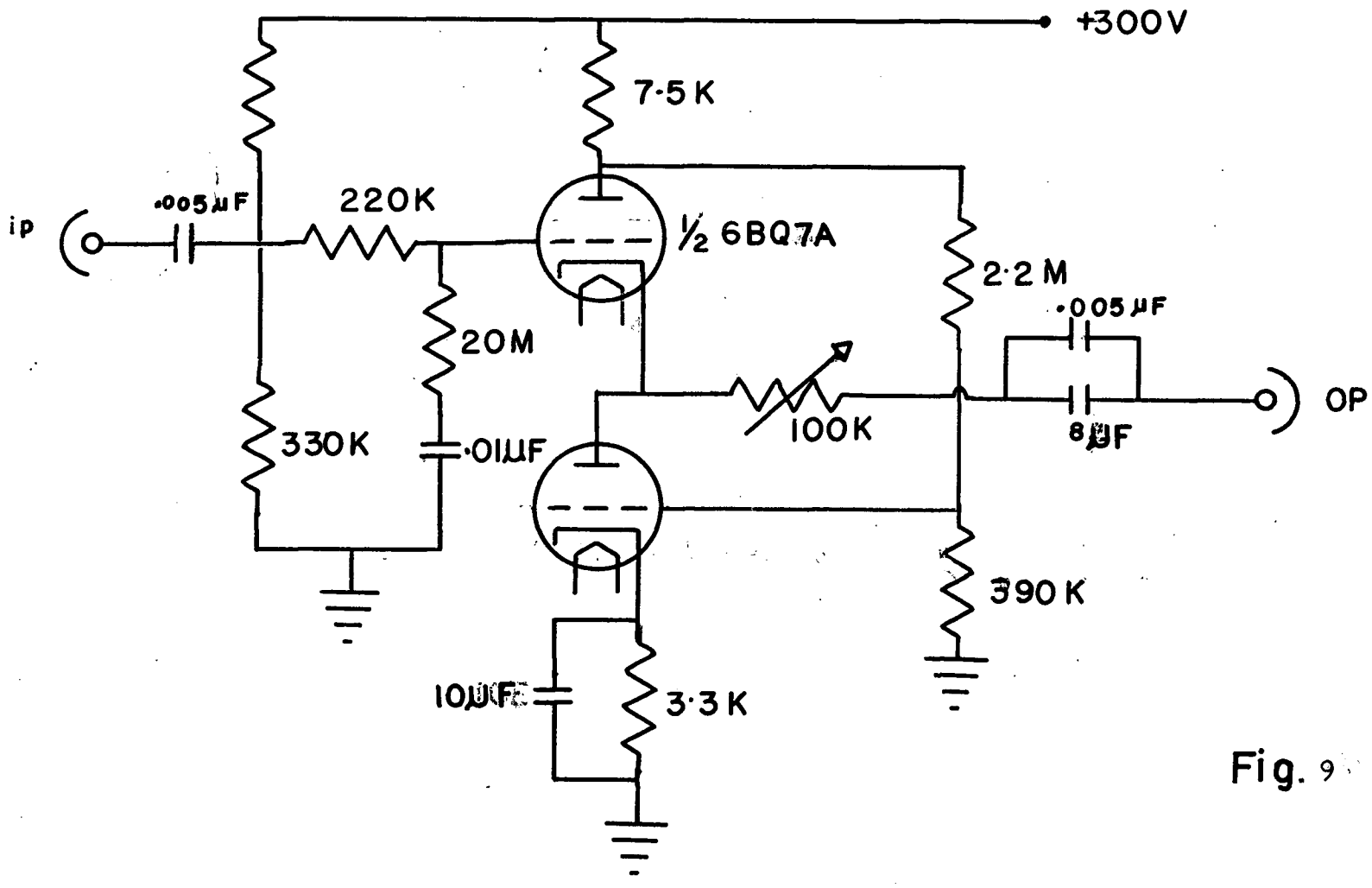

Fig. 9

lower half. This circuit can be regarded as a two tube feed back amplifier.

(VII) Differentiating time constant

The 10 μμF capacitance from anode to ground, Fig. 8, and the stray capacitance 6 μμF and 47 K resistors in series with anode and EHT gives differentrating time constant of about 40 μ sec. in the anode unit of the photomultiplier which is suitable for the ND 101 input circuit.

Draper and Hickock (1958) and Swank and Buck (1952) have discussed the effect of the choice of differentiating time constants on resolution; this is important when comparisons are to be made between scintillators of different decay times. A kicksorter records the maximum height reached by a pulse. It is only electrons that arrive before the maximum is reached which contribute to the final signal and if the differentiation time is short compared with the decay time of the light pulse, then electrons arriving before maximum contribute to it with unequal weights. The effect of this is to give different variances to pulses of otherwise equal mean size from different light sources. If comparisons are to be made of absolute light outputs both these effects are important. For comparison of resolution, only the second matters. In the present experiments the joint choice of long photomultiplier anode time constant and delay line clipping ensures that no distortion of data occurs. Every electron arriving before the pulse height maximum is reached is recorded with equal weight and no electrons are recorded after pulse height maximum. Although the

fraction of such lost electrons will depend on the decay time of the light pulse, the remainder are still subject to Poisson statistics and provided the pulses are adjusted to have the same mean height at the output, they will have the same variance. The short clipping time also minimizes the effects of "after pulsing".

(VIII) Computations

Computations were carried out on the University of British Columbia Awac III E computer and also on the I.B.M. 1620 at the University of Alberta, Calgary by Dr. J. R. Prescott. Means and variances were computed from the complete data and not estimated, for example, from full width at half height of a peaked frequency function.

CHAPTER IV

Procedure and results

4.1 Noise and multiplier statistics

The statistical contribution of the dynode structure alone can be inferred by studies of tube noise, a fraction of which, though not all, arises from single electrons falling on the first dynode. Various authors - Morton and Mitchell (1948), Wright (1954) Roberts (1953) and Breitenberger (1955) have dealt with the statistics of multiplication in general terms. Assuming Poisson statistics for electron multiplication at each stage, Lombard and Martin (1961) have recently evaluated single electron pulse height distribution on a computer. The found peaked distributions, the location of the peak in relation to the mean pulse height being determined by the stage gain. These authors remark that, in fact, the observed noise spectra in actual photomultipliers resemble a decreasing exponential and are not consistant with the Poisson model of secondary electron emission. Observations leading to a similar conclusion are reported by Allen (1950) and Baiker (1960) in a detailed study of tube noise, finds quasi-exponential noise spectra using R.C.A. tubes and in the present work monotonically decreasing noise spectra, have always been obtained, frequently almost exponential over several decades and usually showing a second component (see examples in Fig. 11 and 12). Livessey (private communication) finds considerably more complex noise spectra, often having three or more distinguishable components, in an EMI type 6099B of "Venetian blind" structure.

In so far as the mechanisms giving rise to noise in photo-

multipliers are still not properly understood (see e.g. Baicker (1960)) the only satisfactory way at present of constructing a model for multiplier statistics is to make actual measurements of the noise spectrum under the prevailing conditions on the tube being used. Since the tube noise does not arise exclusively from electrons originating at the cathode, it is necessary to distinguish this component from others by allowing a weak continuous light to fall on the cathode and subtraction to determind the noise distribution of interest. This is discussed in more detail in subsequent sections.

In the following sections the foregoing analysis is first tested with no special assumption about the statistics of multiplication process. Experimental observations of the frequency function of output pulses are then compared with predictions based on specific models for the multiplication process. In both these sections, the light pulse were produced by an artificial light pulser described earlier. Finally, observations on actual scintillation assemblies are related to the ideal cases discussed later.

4.2 Noise and resolution

Measurements were first made with the light pulser described earlier to test the validity of expression (2) and hence of the initial assumptions for the derivation of the statistical model outlined in Chapter II, (2.1).

The mean voltage signal on the photomultiplier anode is $G = n \tau me/C$ where C is the anode capacitance, m the multiplication of

Relative variance as function of reciprocal pulse height at different focus settings

curve (a) 7046

(b) 6810 A

(c) curve (a) corrected for single-electron spectrum changes

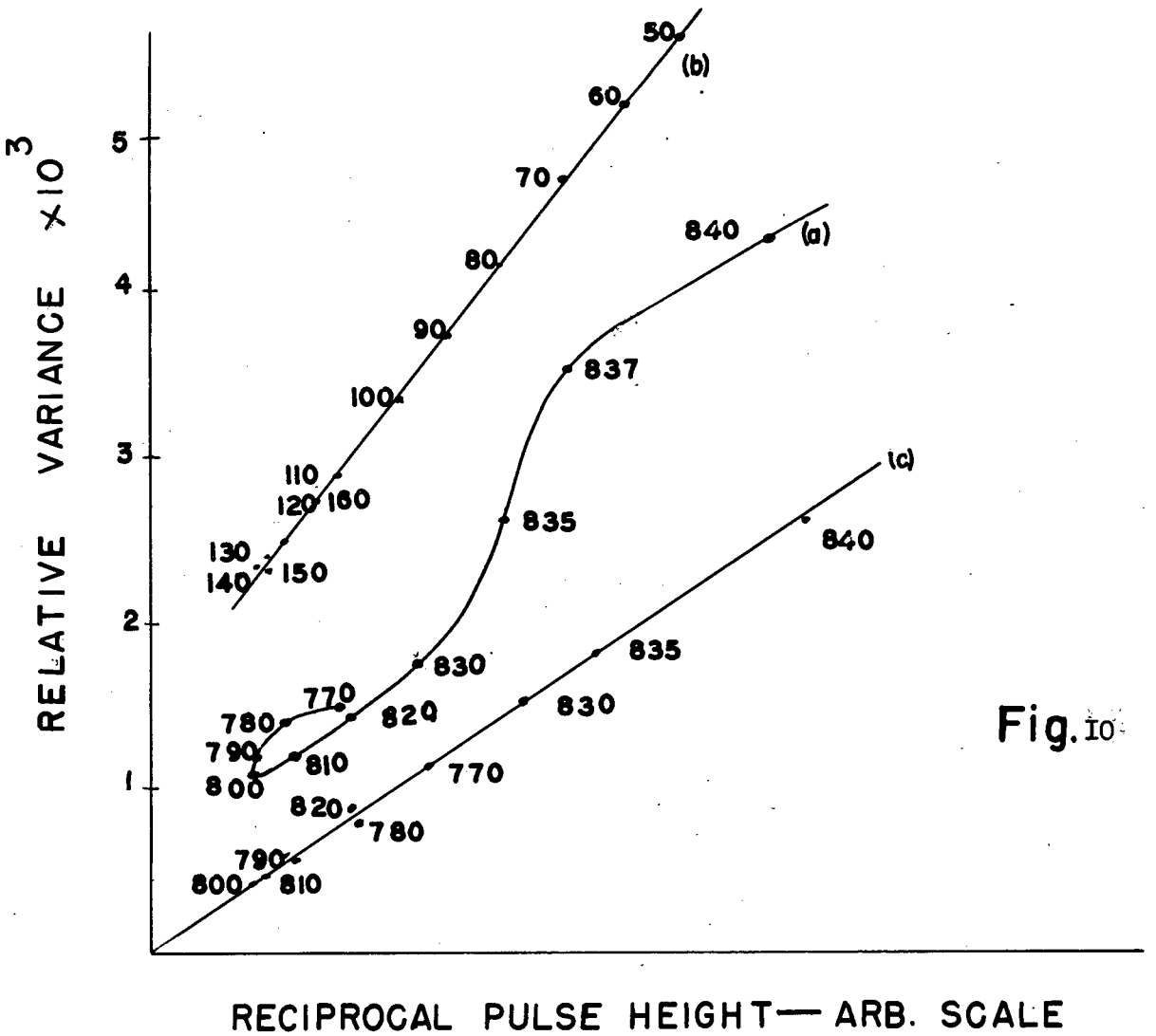

Fig. 10

the tube and ē the electronic charge. Equation (2) becomes:

$$V_G^* = G^2/M^2_G = m\ e\ (1 + Vm)/G_{MG} \qquad (9)$$

Thus provided Vm and m remain constant, V_G is proportional $1/\mu_G$.

This relationship was repeatedly tested in the course of experiments. In some scores of instances with different photomultipliers, widely different conditions of applied voltage and focus, and with cathodes fully and partially illuminated, no case was found where V_G was not strictly proportional to $1/\mu_G$, see for example, Fig. 18. This result has, of course, been found by many observers. It is concluded first, that assumptions of Poisson light production and binomial transfer are valid and second, that there was no significant contribution to the variance from "instrumental" resolution other than the photomultiplier itself.

When the pulse height was varied by variation of the focus voltage above, however, the somewhat unexpected results displayed in Fig. 10, (Curves (a) and (b) were obtained). The most obvious effect of focus variation is to change the transfer efficiency and with it the mean pulse height. While the general trend for relative variance to decrease with increasing pulse height is maintained, the curves particularly that for the 7046 tube, display some curious anomalies. For instance, in the 7046 the focus setting for maximum pulse height does not coincide with the setting for best resolution and the curve displays double values in this region. The plot for the 6810A has a non zero intercept on the V axis. This behaviour is accounted for by

changes with focus setting of the multiplication and its relative variance. These can be assessed by measurements of the pulse height distribution of the tube noise, or more accurately, that portion of the tube noise which originates at the photo-cathode.

Fig. (11) shows a set of noise spectra for the 7046 obtained under conditions of weak continuous illumination from which noise under dark conditions has been subtracted. The change in the character of the distributions with focus setting is quite evident. The relative variance Vm of each of these curves is the Vm of expression (6) and the mean is proportional to the multiplication m. The measured mean ranges from 12.5 channels at focus 840 V where Vm is 1.7.

From expression (6) we define $V_G^* = V_G/m(1 + Vm)$ which should be proportional to μ_G^{-1} and this quantity is plotted in Fig. 10 as curve (c); the original curve (b) is now transformed into a straight line through the origin. Such deviations from a straight line as still occur can be attributed to the fact that the behaviour of the noise spectra near the origin is uncertain, to the extent that an extrapolation of 2 or 3 channels is required in this region since the Kicksorter does not record in these channels at the moderately high counting rates involved here, about 30,000 C/sec.

A similar transformation on the curve (b) Fig. 10 for 6810A tube also yields a straight line through the origin although in this case changes in the focus setting principally affect m and leave Vm virtually unaltered. No satisfactory explanation for this behaviour of the tube noise with focus setting has been found. It appears, however, that the theoretical treatment

of Chapter II (2.1) is well supported by experiment.

Although the main concern of the investigating of the tube noise as such was to identify correctly the portion due to single electrons arriving at the first dynode from the cathode, one or two general features of the behaviour of the noise appear worthy of further comment.

It has already been remarked that most of the noise spectra display two clearly distinguishable components: a "steep" quasi-exponential at small pulse heights - see Fig. 12 - and a tail. Single electron pulses released from the photocathode by light fall in the "steep" region of the distribution.

In the tubes discussed here (R.C.A. 6342, 6810A and 7046) the tail typically contains about 2% of the total noise pulses at room temperature and has a logarithmic decrement between five and ten times larger than that for the smaller pulses. It is important to establish whether this tail is associated with illumination of the photo-cathode, for although these pulses are of relatively low abundance, they extend to quite large pulse heights and could significantly increase the relative variance Vm.

Such pulses are not, in fact associated with illumination of photo-cathode for as curve (b) in Fig. 12 shows, only the steep portion of the distribution is increased by permitting light to leak on to the photo-cathode. Further, the temperature dependence of the tail makes it doubtful whether it even originates on the photo-cathode. When the cathode is suddenly cooled by dumping a load of dry ice upon it, the steep component immediately begins to decrease, reaching an equilibrium at about 40 minutes.

Single electron spectra in a 7046 photomultiplier with focus settings as a parameter.

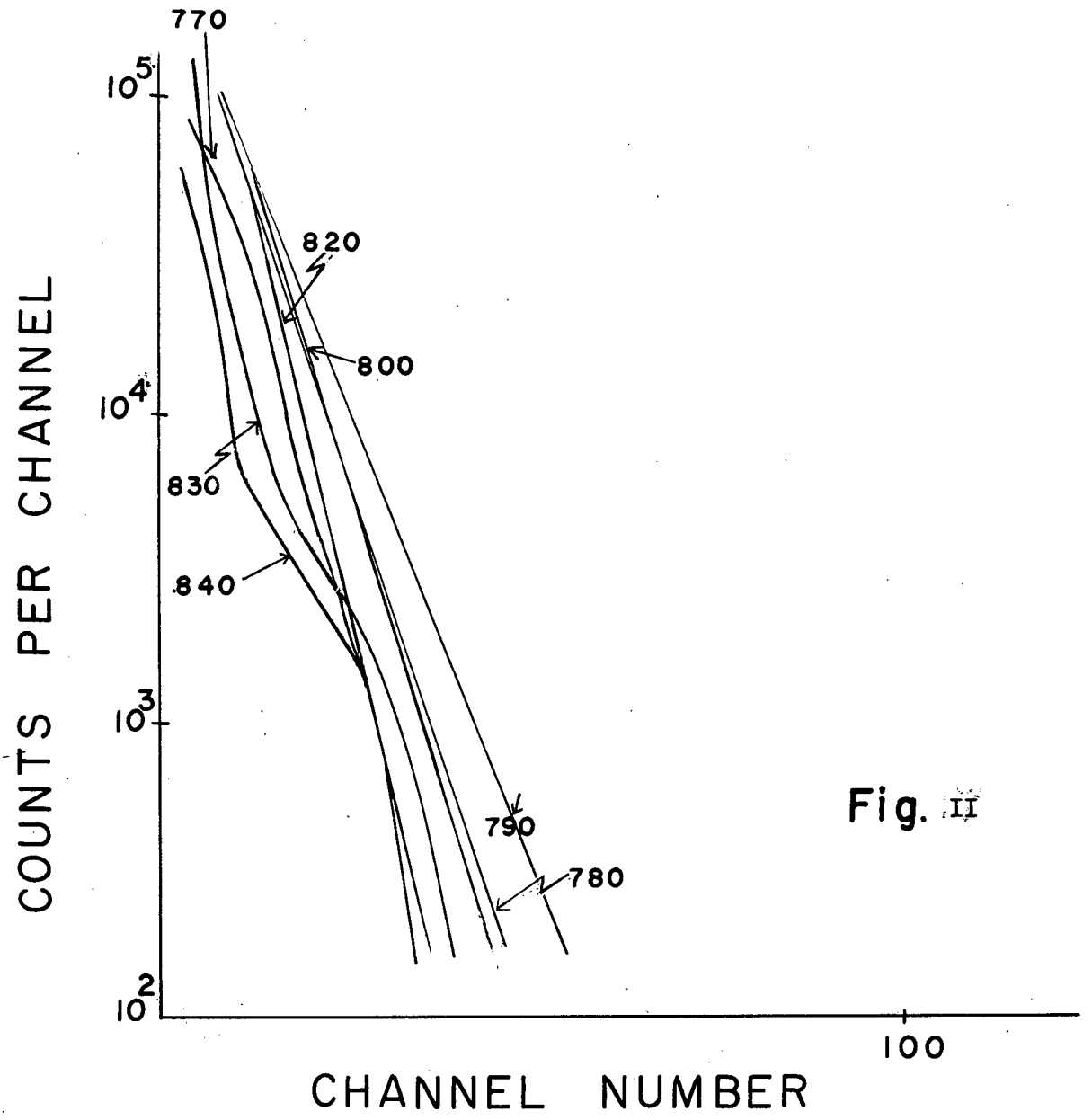

Fig. II

The tail, on the other hand, remains almost unchanged for about 15 minutes. Similarly, cooling of the body only of the photomultiplier first produces a reduction in the tail, while it is the steep part of the noise distribution that now lags behind. When the cathode of a photomultiplier (already cooled around the body) is then cooled, no significant further reduction of the tail occurs, although the "steep" component is almost suppressed. Dr. J. B. Warren suggested that it could be residue gas effect. Curves illustrating temperature effects are also shown in Fig. 12, curves (b) and (e).

Changing the focus setting also changes the relative proportions of the two components in the noise. At settings remote from those which could be regarded as normal operating conditions (high gain, good resolution), the tail becomes much less prominent and eventually disappears. Under these conditions (see Fig. 11) the single electron spectrum itself changes radically in character.

These observations suggest that the tail of the noise distribution originates somewhere inside the photomultiplier, in front of the first dynode, perhaps on the walls of tube or in the focussing structure itself.

Baicker (1960) has observed essentially similar behaviour in a variety of R.C.A. photomultipliers. He interprets the tail as due to bursts of more than one electron from the photo-cathode. While the evidence does not perhaps conclusively eliminate the photo-cathode as the source, it seems certain that it is not produced by light. By fitting the distribution curves discussed in the theoretical section to the tail one

Noise spectra in a 7046 photomultiplier showing the effects of cooling and continous illumination of the photo-cathode.

(a) room temperature phototube dark

(b) " " weakly illuminated

(c) tube body cooled to dry ice temperature

(d) entire tube cooled

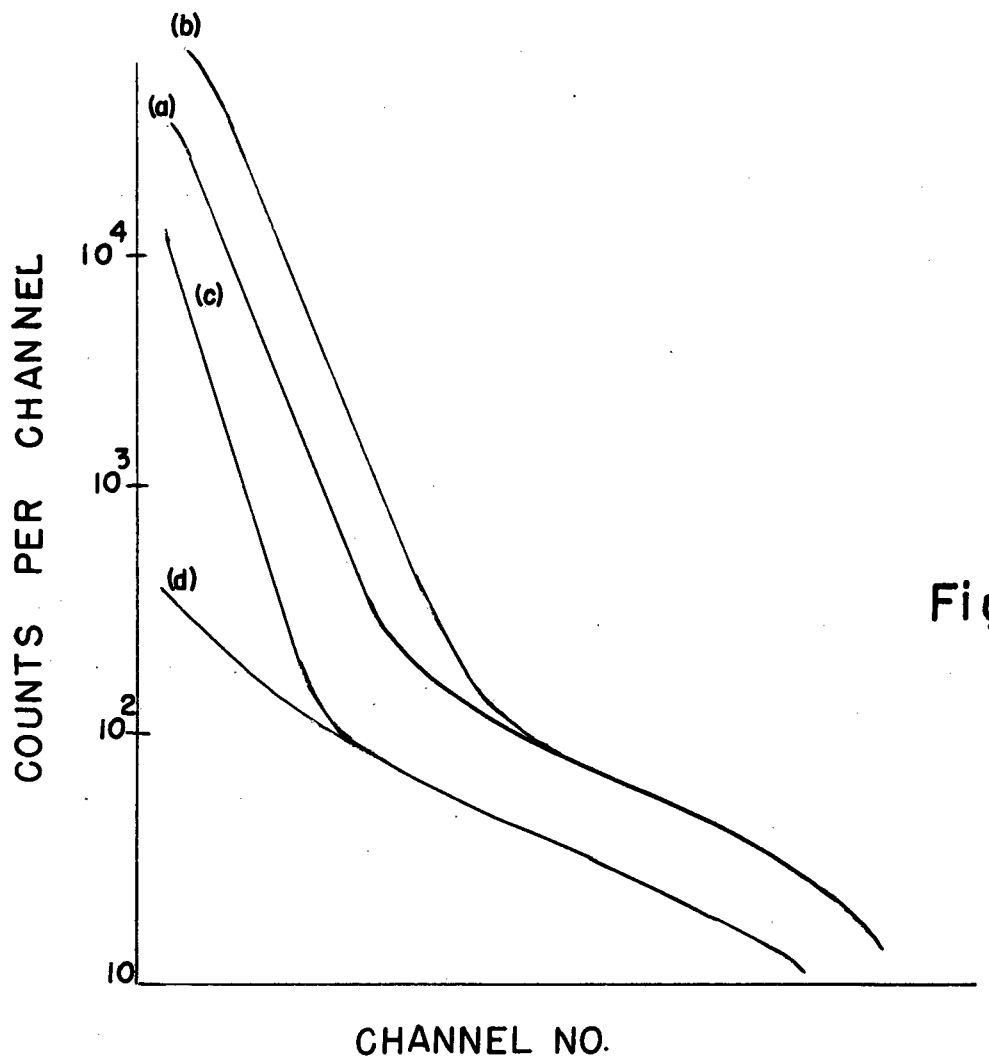

Fig. 12

can estimate that at least five and possibly more electrons would be required.

A few bursts of low multiplicity (2 or 3) might be expected to occur on a basis of chance coincidence. In fact, if an increasingly strong light leak is used, the noise spectrum changes its shape in a manner quite consistant with the increasing occurance of events of multiplicity of two. Even the strongest light source used, however, failed to affect the tail itself in any way.

So far, then, as noise is concerned, a satisfactory empirical model for the statistics of multiplication of single electrons released from the photo-cathode by light can be found and such a model gives fairly good agreement.

4.3 Non exponential Single-electron Distributions

Although the spectrum of single electron pulses can be made fairly accurately exponential in the case of the 7046 photomultiplier, this is an artificial state of affairs and in practice the frequency function of single-electrons exhibits some degree of curvature, although it usually approximates to a simple exponential.

Several alternatives for the single-electron frequency function have therefore been considered and it seemed reasonable to choose models that contain the simple exponential as a special case, viz

$$f(x) = pa^{-1} \exp(-x/a) - (1 - p)(ab)^{-1} \exp(-x/ab) \qquad (9.1)$$

$$f(x) = a^{-1} \exp(-(x/a)^{\xi}) / \Gamma(1/\xi + 1)/\xi) \qquad (9.2)$$

$$f(x) = x^{\xi} \exp(-x/a)/\Gamma(-1)a^{\xi + 1} \qquad (9.3)$$

The first two distributions reduce to simple exponentials if p or ξ is unity; they are more concave than the simple exponential for p or $\xi < 1$, and less concave for p or $\xi > 1$. In the present experiments, either (9.1) or (9.2) was sufficient to represent the observed single-electron distributions, and no case was found where the distribution could be satisfactorily represented by (9.3).

Although the characteristic functions for the system as a whole can be written down for these models, the corresponding Fourier transforms have not so far been found. However, the required frequency function can be found with sufficient accuracy by Edgeworth's series expansion (Cramer (1946)) as follows:

The generating function for the output is (in the notation of Chapter 2)

$$G(\theta) = \exp(-N) \exp(NG_m(\theta))$$

where $G_m(\theta)$ is the generating function for the multiplication process. The amount generating function is obtained as usual by replacing $\log \theta$ with θ .

$$M(\theta) = \exp(-N) \exp(N.M_m(\theta))$$

Since $G_m(\log \theta) = M_m(\theta)$, the moment generations function for the multiplication process is, taking logs,

$$\text{Log } M(\theta) = -N + NM_m(\theta))$$

Since the derivatives of $M_m(\theta)$ are the moments (M) about the origin of the single electron distribution itself the cumulants γ_ν of the distribution are then found as the derivatives of log $M(\theta)$ with respect to θ , evaluated at $\theta = o$. It is seen that the cumulants are just N

Pulse height distributions for a pulsed light source with a 6810 A photomultiplier and a non-exponential single electron distribution; fitted as described in the text.

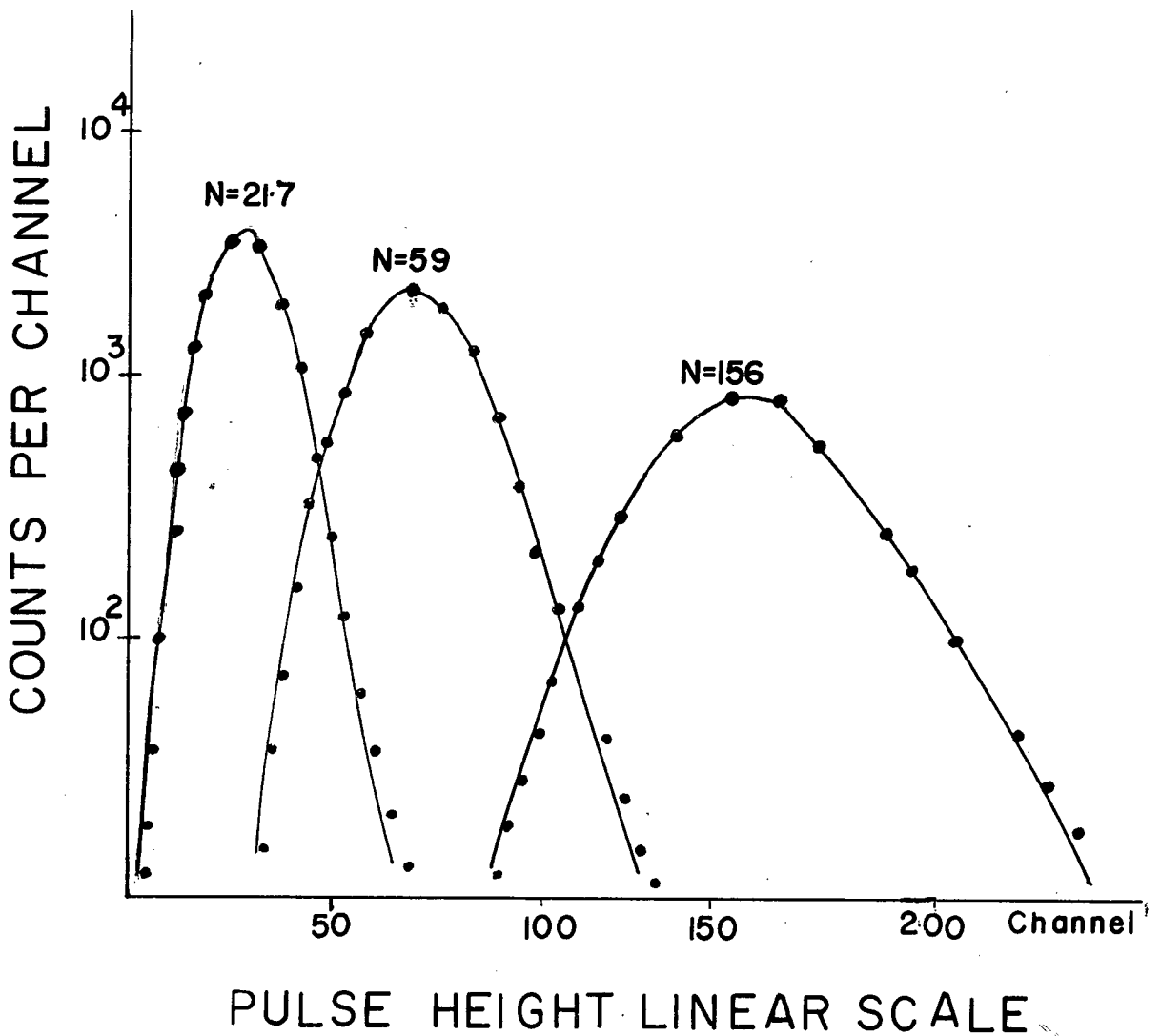

Fig. 13

times the moments about the origin of the single-electron distribution. If we denote the ν th central moment of the complete distribution by M_ν and the mean by μ then:

$$\chi_1 = \mu_1 \; ; \; \chi_2 = \mu_2 ; \quad \chi_3 = \mu_3 ; \quad \chi_4 = \mu_4 - 3\mu_2^2$$

Introducing the standard variable $z = (x - \mu)/\sigma$, we can write the required frequency function (to terms of the order N^{-1}) as:

$$f(z) = \phi^{(0)}(z) - \frac{1}{3!}\frac{3}{\sigma^3}\,\phi^{(3)}(z) - \frac{1}{4!}\left(\frac{\mu_4}{\sigma^4} - 3\right)\phi^{4}(z) - \frac{10}{6!}\left(\frac{\mu_3}{\sigma^3}\right)^2 \phi^{(6)}(z) + \cdots$$

where $\phi^{(i)}(z)$ is the ith derivative of the standard normal distribution. Using distributions (9.1) and (9.2), the vth cumulants are respectively:

$$N\nu!\, a^\nu (b + b^\nu (1-b)) \quad \text{and}$$

$$N(\nu+1)^{-1} a^\nu \Gamma((\nu + 1 + \xi)/\xi) / \Gamma((\xi+1)/\xi)$$

The parameters in these distributions are best found by trial and error or direct computation from the single electron frequency function since the form of these functions does not encourage estimation of the parameter by the usual, e.g. maximum likelihood or least squares.

In the course of the search for suitable models to describe non-exponential single-electron distributions, an interesting and useful approximation was discovered. Equation (6) can be rewritten $G^2/\mu_G = M(1+Vm)$ where M is the mean pulse height for a single electron. For a simple exponential this becomes $\mu_G^2/\mu_G = 2a$ where a the mean single-electron distribution is clearly non-exponential, by interpreting the ratio $\sigma_G^2/2\mu_G$ as if the statistical model for multiplication were a simple exponential, viz interpreting M as equal to $\sigma_G^2/2\mu_G$. This is equivalent to interpreting a in expression (6) merely as a scale factor given by $a = \sigma_G^2/2\mu_G$. Suppose, for example, that Vm is less than unity. The approximation will then clearly underestimate M and overestimate $N = \mu_G/M$,

Pulsed height distributions for pulsed light source with simple exponential single electron distribution in a 7046 P.M. solid curves are computed from expression (4) in the text N values are given for each curve.

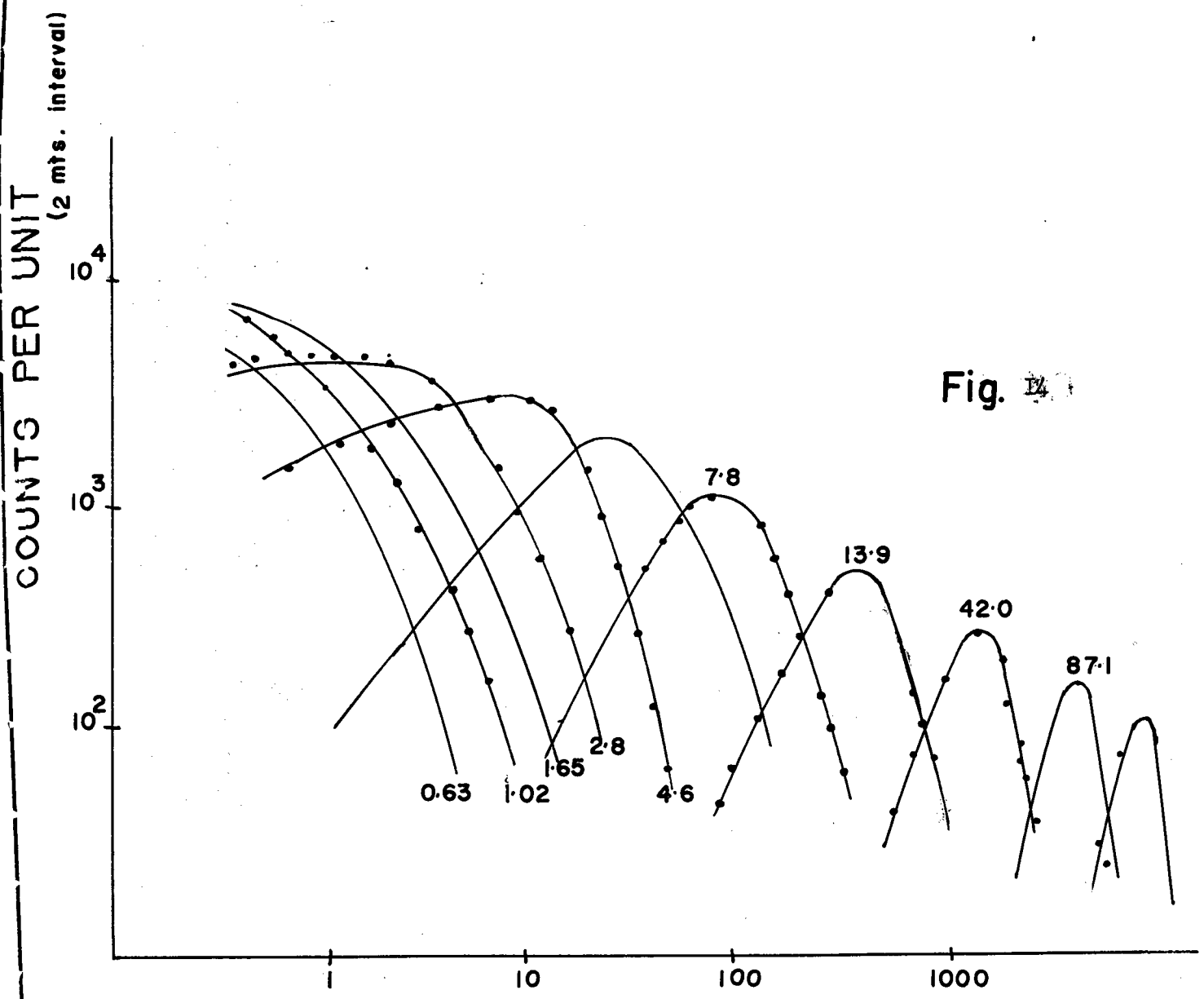

Fig. 14

the mean number of electrons at the first dynode. However, this is exactly compensated for by the greater variance of the exponential distribution and the resulting frequency function turns out to represent the actual frequency function to a remarkable degree of accuracy. As example is shown in Fig. 13 where three curves for the 6810A are shown fitted in this way. The single-electron distribution for this case was of the type (9.2) with $\xi = 2.1$ and $Vm = 0.53$. The above procedure guarantees, of course, that at least the mean and variance are correct. In the particular examples shown in Fig. 13, the third moment was within 10% of its correct value and the fourth moment within 20%.

This happy accident has much relieved the tedium of calculating distributions using Edgeworth's series, (itself an approximateion) although there is no guarantee that it will necessarily work in all cases.

4.4 Experimental verification of the shape of the ideal Scintillation line:

The relations (4) and (5) in the first chapter were tested using 7046 photomultiplier. By means of the focus control the noise spectrum was adjusted to be as nearly a simple exponential as it was possible to make it. By a graphical test the distribution was exponential over three decades. Because of loss of counts in the first four kicksorter channels the noise spectrum was not certain in the region near the origin but it was assumed to be exponential.

Light pulses were produced by the pulse generator described in the section "Electronics" operating at 1000 c/sec an average of less than ten electrons at first dynode, the tube pulses become confused with the noise of the photomultiplier itself. To separate the two sources of

Variance vs mean for pulsed light signals with a simple exponential single electron distribution. 7046 photomultiplier.

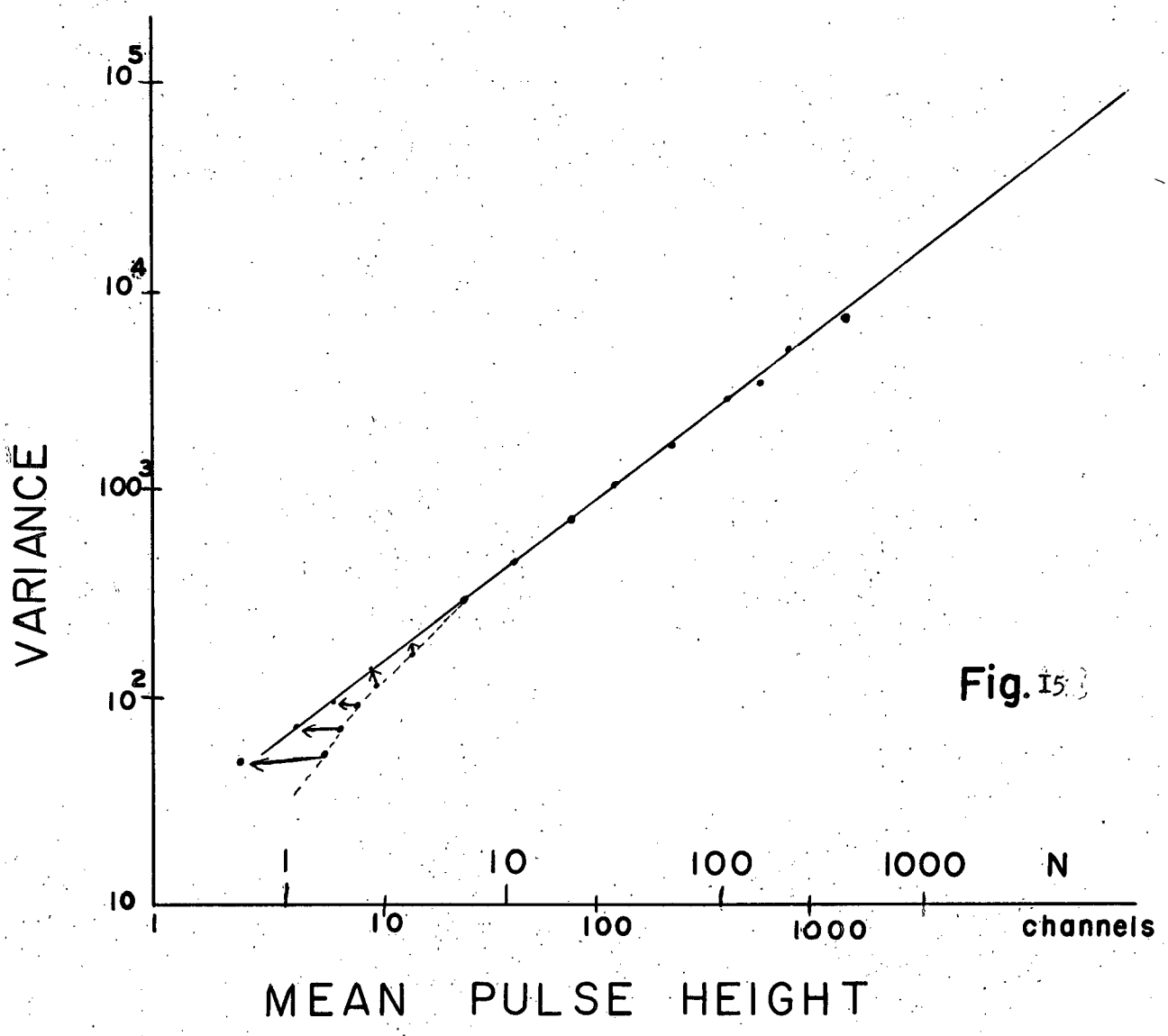

Fig. 15

signals, the light signals were admitted to the kicksorter by a gate opened by the same signal that drove the light pulser, as shown in Fig. 16. In this way except for those pulses occuring by chance during the time the gate is open, noise is excluded. With a photomultiplier operated at room temperature, these randomly-gated noise pulses nevertheless constitute a problem, for although only 4.5% of the noise pulses themselves occur while the gate is open, the noise count-rate is high and in fact, some 20% of the gate pulses are accompanied by an analysed noise pulse. In terms of the complete assembly, consisting of the light source, the photomultiplier and analyzer this means that a significant fraction of the signals due to light pulses are accompanied by a random noise pulse within the resolving time of the pulse height analyzer. To reduce the contribution of random noise pulses to a negligible level the photomultiplier was cooled to dry-ice temperature. Under these conditions less than 3% of gate pulses are accompanied by an analysed noise pulse.

A second function of the gate signal is to give an estimate of the proportion of cascades that fail to start. For each run, the number of gate pulses was recorded on a scaler and compared with the number of pulses actually analysed. If k is the fraction of pulses lost and if we denote by subscripts the measured mean and variance, then the true mean and variance, μ and σ^2 respectively, are given by:

$$\mu = (1 - k)\,\mu_1$$

$$\sigma^2 = (1 - k)\,(\sigma_1^2 - K\mu_1^2)$$

and the relative variance V by:

$$V = (V_1 - k)/(1 - k)$$

Figure 15 shows the variance plotted against the mean for light signals. Logarithmic scales are used to cover the wide range of pulse

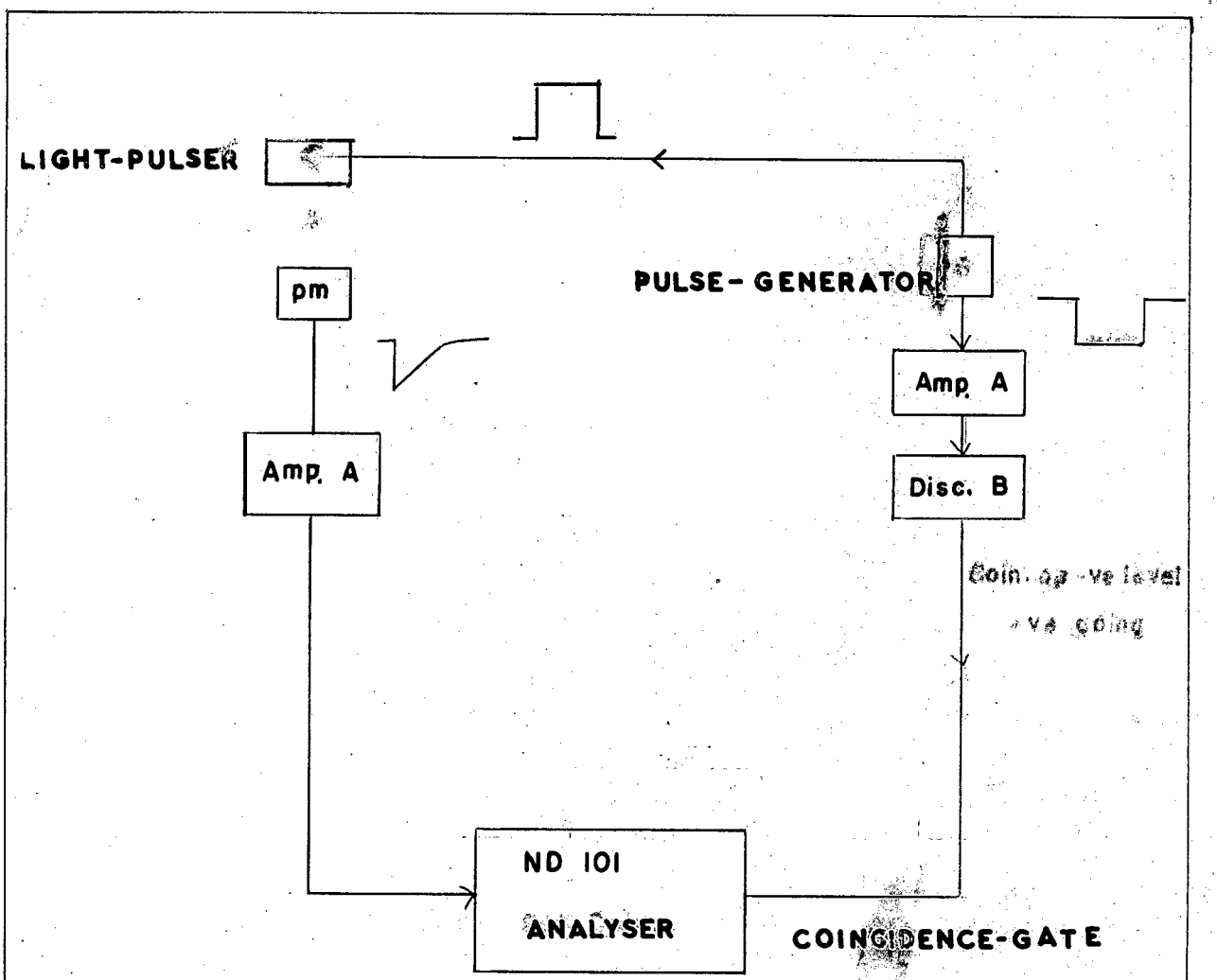
LIGHT-PULSER
pm
PULSE-GENERATOR
Amp. A
Amp. A
Disc. B
ND 101
ANALYSER
COINCIDENCE-GATE

Fig. 16

heights and variances encountered. At low mean pulse heights the correction has been made for cascades that fail to start and the extent of this correction is indicated by the arrows attached to some of the experimental points. The points are fitted by a straight line of slope unity, showing that the variance is proportional to the mean, the proportionality constant being 11.4 $\pm$ 0.1 channels, corresponding to a value of $\underline{a}$ of 5.7 $\pm$ 1% channels. This is to be compared with the value 6.0 $\pm$ 0.2 channels obtained for $\underline{a}$ from the slope of the noise distribution. This agreement must be considered satisfactory, since measurements of $\underline{a}$ based on the noise distribution were reproducible only to about 3% during the course of the series of measurements. A scale of values of N using $\underline{a}$ = 5.7 is shown in the figure. Actual frequency functions were calculated using 5.7 channels for the value of $\underline{a}$ and normalising the areas to the total count. These distributions are shown in Fig. 14. It is worth observing that curves are not fitted individually except insofar as the appropriate value of N for each was found from the relation μ = Na. Here again the agreement between the observations and the computed distributions is very satisfactory. In Fig. 14 the logarithmic abcissa scale conceals the skew character of the distributions which is quite evident on a linear plot even for large values of N. Thus a reasonably satisfactory set of statistical models has been found to describe the performance of the photomultiplier in a scintillation assembly. In particular, expression (4) can probably be regarded as a sufficiently good representation of the shape of the ideal scintillation line even in cases where the simple exponential model from which it was derived is not applicable. It is nevertheless "ideal" in the sense that

RESOLUTION DATA FOR LIQUID SCINTILLATOR

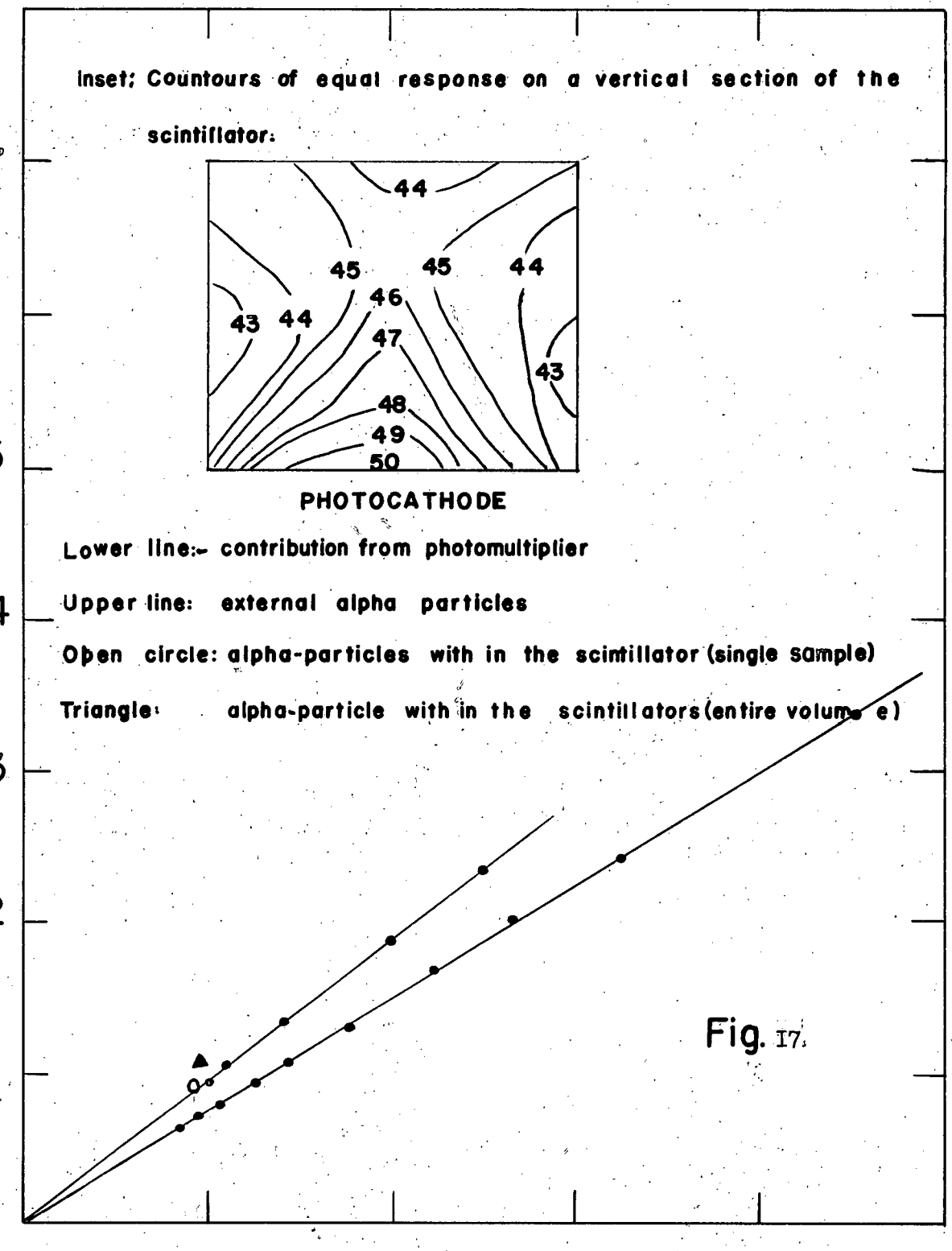

Fig. 17.

it takes no account of variations in transfer probability. However, in some cases it does fairly adequately represent the line shape in practical scintillation counters, for example, in the case of alpha-particle excitation of a liquid scintillator and perhaps also for gamma rays of very low energy in sodium iodide. It is just in these cases that the skew character of the distribution is significant. For large signals the distribution is effectively Gaussian.

4.5 Transfer effects in an organic Scintillator

In order to estimate the magnitude of transfer effects contribution, described in Section 2.3, Chapter II, the spread of pulse heights from different regions of a liquid scintillator, NE 219, was determined by immersing in it a small alpha-particle source.

To isolate transfer effects specifically, the response of this scintillator to an external source of alpha particles was first determined. For this purpose it was incorporated in a glass cell 1.5" in diameter, filled to a depth of 0.7 cm. and optically coupled directly to the photo cathode of a 6810A photomultiplier. An aluminium reflector surrounded the cell inside the walls and a plane reflector was held just above the surface of the liquid. Alpha-particles were incident on the free surface of the liquid through a small hole in the upper reflector, and were varied in energy by adjusting the distance of the source from the liquid surface. The hole in the reflector was kept sufficiently small (3 mm in diameter) to eliminate the need for solid angle corrections. It was hoped that by confining the alpha-particle to a very small area on the top surface of a relatively large volume of scintillator that geometrical light collection factors would be the same for all scintillations. The alpha-particle source

used was prepared as described earlier in Section 3.5, Chapter III. In order to avoid corrections for alpha-particle range straggling, the minimum alpha-particle energy used was about 3 MeV where the contribution from straggling to the relative variance is about 3×10^{-4} (Evans) (1955).

The results for alpha-particles on liquid scintillator are shown in Fig. 17 (upper curve) where relative variance is plotted against reciprocal mean pulse height. The points are consistant with a straight line through the origin. For comparison purposes a corresponding curve for the artificial light pulser, representing "ideal" resolution is shown. It is clear that the relative variance of the liquid scintillator is some 25% greater than for "ideal" pulses of similar mean pulse height. Because of the source geometry it seems unlikely that this increase could be due to variations in the light collection efficiency. Whether it is a consequence of the use of the heavily ionising alpha-particles or is a property of the scintillator in the sense of an intrinsic resolution, unfortunately cannot be determined from the present experiments.

Transfer effects <u>within</u> the liquid scintillator were then investigated by filling the scintillation cell to a depth of 1 - $\frac{1}{4}$ inches and immersing in it a small alpha-particle source that could be moved from place to place as described by Cummins and Delaney (1960). This source was Po^{210} deposited on the end of a length of silver wire, 0.030 inches in diameter, for a distance of about 1 mm. The source wire passed through a hole in an oversize, plane, aluminium reflector resting across the top of the cell. The reflector was constrained to allow lateral movements of the source and completely covered the top of the scintillator cell at all times.

With the source within the scintillator and at the geometric centre of it, the point represented on Fig. 17 by an open circle was obtained. Because of the small size of the source, with a single reading of this type, the transfer variance should be small and the point should lie very close to the line obtained with external alpha-particle excitation, even though the source is now inside the scintillator. This is seen to be the case.

Readings were now taken of mean pulse heights in planes parallel to the surface of the scintillator from the base of the cell until the source began to emerge through the surface. The extreme variation between different points in the scintillator was about 20% and the relative standard deviation 4% (relative variance 17×10^{-4}, 180 sampling points). An independent check of this figure was obtained as follows:
A strong Polonium source was prepared and left in the scintillator for 24 hours. In this period, the liquid became fairly heavily contaminated. The source was then removed and the pulse spectrum from the contaminated scintillator observed. This contains contributions from all parts of the volume and should have a correspondingly increased relative variance. This experimental point is shown as a triangle in Fig. 17, it lies above the former curve by 18×10^{-4} which is to be compared with 17×10^{-4} obtained in the three dimensional survey. This agreement may be regarded as very satisfactory and it appears that these figures provide a reasonable estimate of the transfer variance for scintillation events randomly distributed throughout the scintillator volume.

It was observed in the survey that the contours of equal response

on a horizontal section of the scintillator followed more or less closely the shape of the sensitivity contours of the photo-cathode obtained by scanning a small light spot over its surface, although the absolute variation from point to point was much less. It seems clear that greater uniformity of the photosurface would have reduced the value of the transfer variance significantly, at least in the present scintillator. Making the cathode less uniform by adjustment of the focus control certainly worsened by resolution, even when correction had been applied for the consequent reduction in mean pulse height. A vertical section through the scintillator showing contours of equal response is shown as an inset to Fig. 17.

It is interesting to observe that in all except the last measurement (contaminated scintillator) the resolution is still close enough to ideal for the distribution curves to be noticeably skewed and for the "ideal" line shape of section 2.2 to be able to give a good fit to them.

When the scintillator is used for the detection of gamma-rays, transfer effects are again expected to be important since ionising events take place throughout the volume of the scintillator. The above survey was used to interpret the resolution observed for uncollimated gamma-rays of energy 0.511, 0.622, 1.28 and 2.62 MeV in the same scintillator, incident on the top surface. The interpretation of resolution for gamma-rays detection in an organic scintillator is not so straightforward as it is in sodium iodide, for instance, because there is no full-energy peak and the resolution must be estimated from the shape of the Compton edge. The following procedure was adopted: Electron energy distributions were computed for each energy: Gaussian resolution functions

Resolution data for gamma-rays in liquid scintillator

Solid circles: gamma-rays resolution

Opencircles: gamma-ray resolution corrected for transfer effects.

Lines A and P are respectively alpha-particle and photomultiplier taken from fig 3

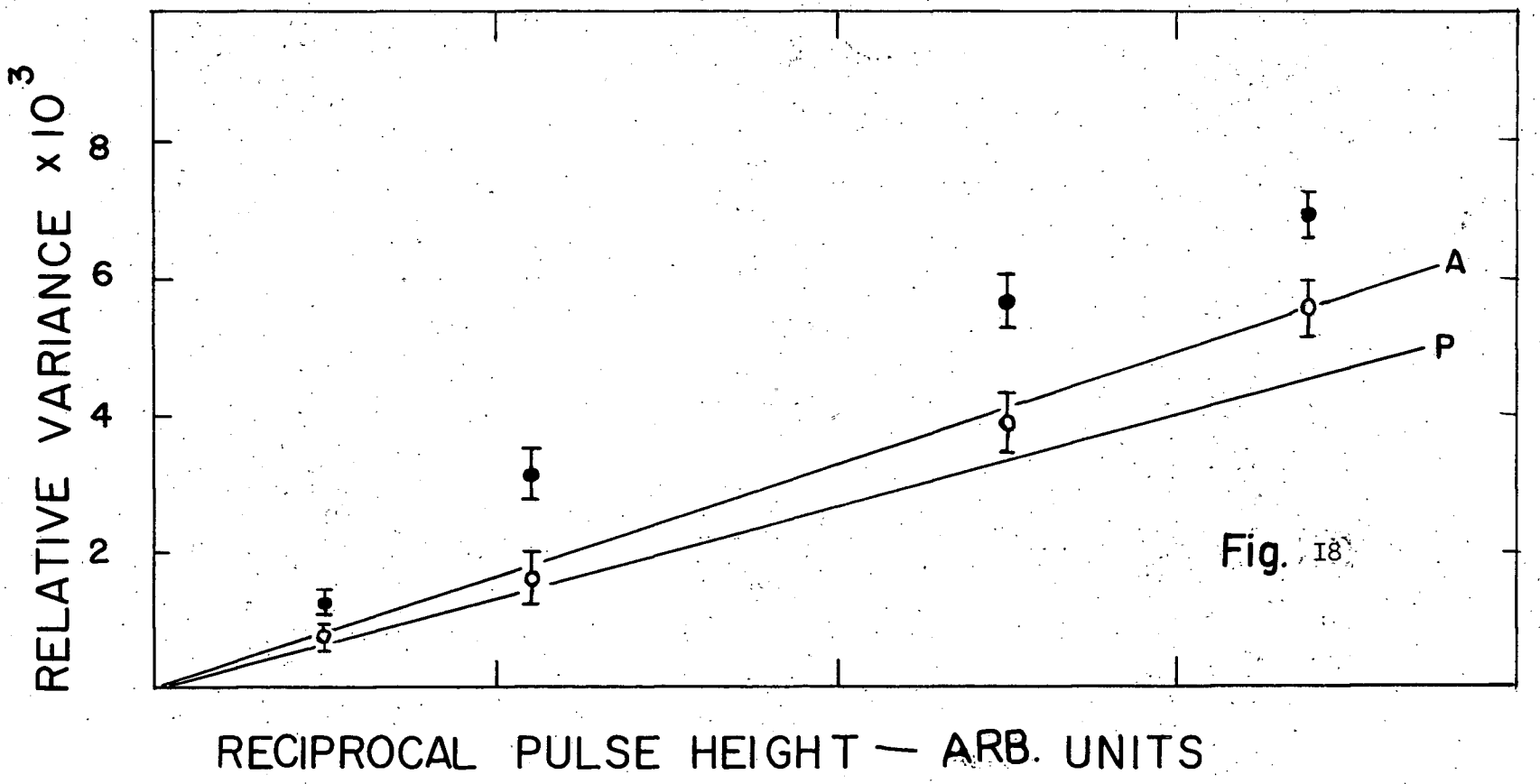

Fig. 18

were then folded in with a range of values of relative standard deviation at the Compton edge. Graphs were then constructed showing the ratio: abcissa at maximum/abcissa at half height versus relative standard deviation. The same ratio was found for the experimental Compton distributions and from the graph the appropriate relative standard deviation. The latter figures, converted to relative variance are shown in Fig. 18 (solid circles) together with the "ideal" photomultiplier resolution line, and the alpha-particle resolution curve discussed earlier. The experimental errors are unfortunately large here because of the method of estimation used and are the standard deviations of 4 measurements for the three upper points and 2 measurements for the lowest (2.62 MeV). The points for gamma-ray resolution lie well above the curve for the same scintillator under alpha-particle excitation and the increase may be attributed to variations in the transfer probability.

The three-dimensional survey of the scintillator was used roughly to estimate the expected contribution to the relative variance from such transfer effects as follows:

Signals at the Compton edge arise from electrons projected straightforward. The pulse heights from the three dimensional survey were therefore averaged over a distance equal to the range of such an electron parallel to the direction of incidence (perpendicular to the surface of the scintillator). No allowance was made for multiple scattering or edge effects. In the case of the 511 and 662 MeV gamma-rays the average was weighted to allow for the exponential absorption of the radiation. In an organic scintillator of this size, multiple interactions can be neglected.

The contributions from transfer effects computed in this way were

subtracted from the experimental relative variances to give the points shown by open circles in Fig. 18. Although these are more consistant with the resolution line for alpha-particles on the liquid than that for the photomultiplier alone, the latter line lies well within the 95% confidence limits for the linear regression fit to the data and no conclusions can be drawn from these measurements about the existence or otherwise if a true intrinsic resolution for this scintillator suggested by the alpha-particle measurements. However, it is correct to say that the major portion of the relative variance is accounted for by a combination of photomultiplier statistics and transfer effects. Edge effects and scattering, neglected here, will produce some further worsening in resolution.

Similar observations were made for an Ne 102 plastic scintillator of the same dimensions, packed in magnesium oxide. Within the (rather large) experimental errors the gamma-ray resolution was the same as for the liquid. Alpha-particle resolution was slightly worse (about 8% in relative variance) but this could be due to surface defects in the solid plastic.

4.6 Transfer Effects in Sodium Iodide

The results for gamma-ray detection in the organic scintillator shown in Fig. 18 are very reminiscent of similar curves for gamma-ray detection in NaI(Tl), (Kelley et al, (1956), Bernstein (1956), Bisi and Zappa (1958), see also Fig. 19). Not only is the trend of the curves with energy similar, but they lie about the same distance above the line of ideal resolution. This originally suggested that the increased line-width in sodium iodide might contain a large contribution from transfer variance and not be due entirely to an intrinsic resolution of the type

Resolution data for gamma-rays in NaI. experimental points are shown solid circles.

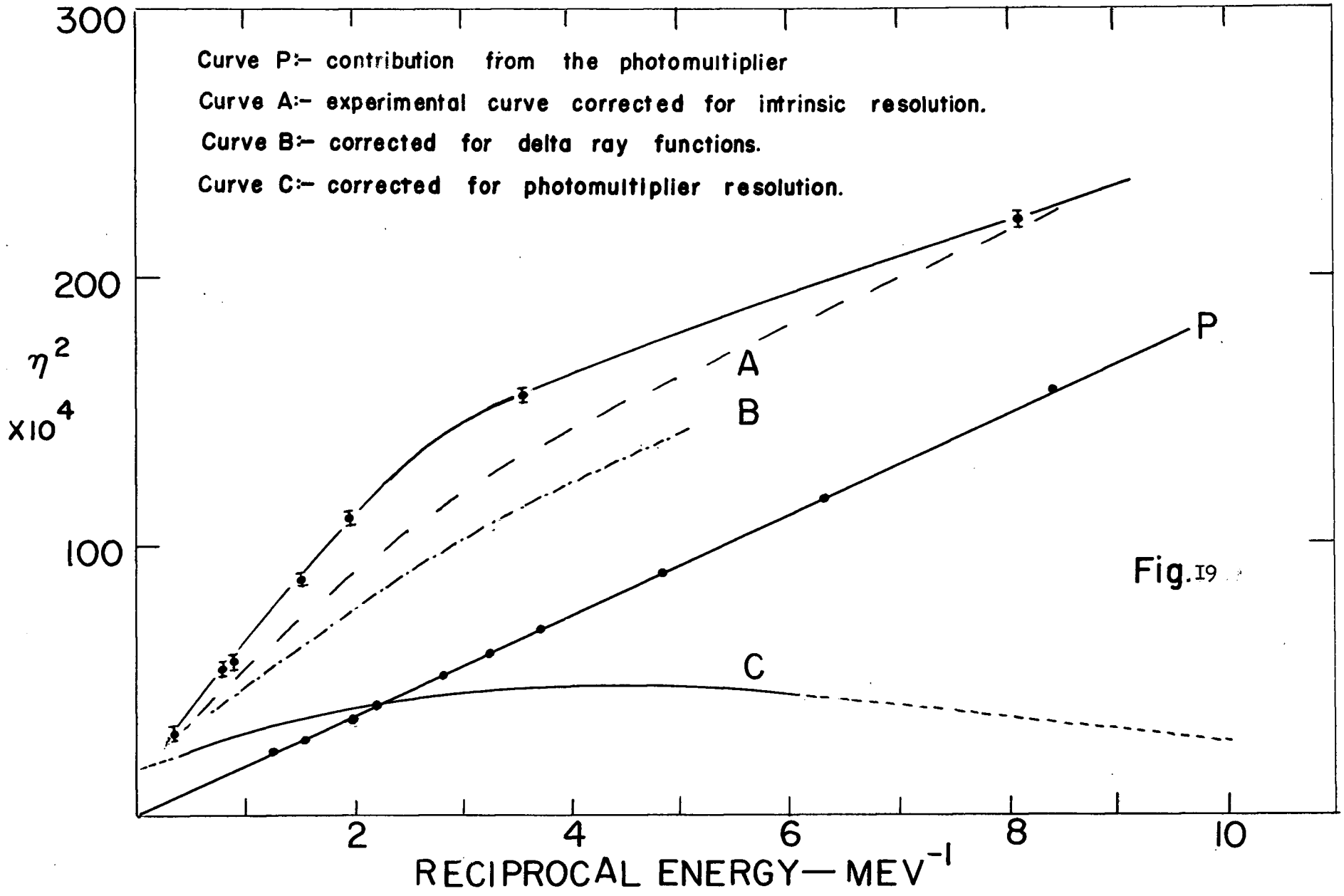

Fig. 19

suggested by Kelley et al (1956). Resolution was therefore measured for gamma-rays in a sodium iodide crystal, 1-$\frac{1}{2}$" diameter, 1-$\frac{1}{4}$" high, mounted on a 6810A photomultiplier and the results are shown in Fig. 19 (solid circles). In this instance the ordinate is the square of the relative full width at half-height of the full-energy peak and not the true relative variance used elsewhere in this Thesis. In order to find the latter it is necessary to have the full-energy peak sufficiently well separated from the rest of the spectrum that a plausible estimate can be made of its shape in the tails of the distribution which have a large influence on the variance. Although an attempt was made to find the true relative variance by estimating the shape of the curve, the results had an unacceptable scatter and the attempt was abandoned. If all the factors that contribute to the line width were strictly Gaussian, N^2 would be related to the true relative variance, V_A by $N^2 = 5.56\ V_A$. Although this will not actually be the case, as the knowledge of these functions is insufficient and Gaussian assumption was used, the quantitative error introduced probably does not exceed the other uncertainties and the qualitative arguments are not affected. The points in Fig. 19 are the means of six determinations and the errors are sample standard errors. The gamma-rays were of energies (in MeV) 2.62, 1.28, 1.11, 0.662, 0.511, 0.279 and 0.123 and they were uncollimated. The curve is essentially similar to those published by Kelley et al (1956), Bernstein (1956), and Bisi and Zappa (1958), except that it does not extend to such low energies. The line P represents the contribution of the photomultiplier itself to N^2 and was obtained using the light pulser.

In addition to the contribution of the photomultiplier, there is the contribution to N^2 from the intrinsic resolution discussed by Zerby, Meyer, and Murray (1961), and Iredale (1961). These two investigations agree well at energies above 0.5 MeV but are in serious disagreement at lower energies. In allowing for intrinsic resolution the results of Zerby et al (1961) as being much more detailed and embodying fewer approximations were preferred. These authors publish curves showing intrinsic resolution as a function of energy and crystal size. It is zero below about 100 KeV where the full-energy peak results almost entirely from a single photo-electric event, rises to a maximum of 5% relative full width at half-height at about 400 KeV and then falls more slowly to about 1% at 3 MeV. No significant variations are found for differing conditions of source-crystal geometry, and for crystals greater than one inch in diameter and height, only a very slow change with crystal size is observed and then only at gamma-ray energies over 0.5 MeV. The intrinsic resolution was taken from Fig. 4 of the paper of Zerby et al (1961,) with a reduction for crystal size from their Fig. 5.

The effect of subtracting this intrinsic resolution from the experimental curve in Fig. 19 is shown by the dashed curve, A. A further source of line-width, discussed by Iredale (1961), is contributed by fluctuations in secondary electron (delta-ray) production. He has computed this contribution for a crystal slightly larger than that used in the present experiments. It is assumed that these figures are valid for our smaller crystal and they have been subtracted

from curve A in Fig. 19 to yield curve B. It is unfortunate that Iredale's results do not extend below 200 KeV and it would be particularly interesting to know the behaviour at lower energies. Finally, by further subtraction of the contribution from the photomultiplier, curve C is obtained. It is clear that a major fraction of the line width remains to be accounted for. We interpret this as due to variable transfer probability. Curve C then represents (apart from a constant factor) the transfer variance as a function of gamma-ray energy. It is instructive to discuss the expected form of this curve, particularly at low energies for which experimental data is lacking: at very low gamma-ray energies, the absorption coefficient is sodium iodide is so large than an overwhelming fraction of the scintillation events take place in the top surface layers of the crystal. Even at 100 KeV, for instance, over 90% of the interactions take place in the top 0.5 cm., mostly by the photoelectric effect. For low energies, therefore, all gamma-ray energies should share a common transfer variance represented by the relative variance in the light collection efficiency across the top surface of the scintillator, with a rise beginning in the region of 100 KeV as the gamma-rays begin to penetrate more deeply into the crystal. If the photoelectric effect were alone responsible for gamma-ray absorption, we should then expect the curve to continue to rise until, for a crystal of the size used here, it levelled off at energies above about 700 KeV at a value equal to the transfer variance taken over the whole volume of the crystal. In the region where the rise would begin, however, multiple events start contributing to the

full-energy peak. The light production is now the weighted average of at least two samples from the distribution of transfer probabilities. it is a well-known statistical result that such an average has a reduced variance. In this case, the variance is reduced by a factor equal to the sum of the squares of the relative energy releases. At higher energies, an increasing fraction of the full-energy peak is due to secondary and higher interactions. At 662 KeV, for instance, roughly 75% of the counts in the full energy peak are due to multiple events as shown by Iredale (1961), Bergerand Doggett (1956), and Lazeu and Davis (1956). The transfer variance is expected to reach a flat maximum and then begin to fall as the above averaging process takes over. In the present crystal the maximum appears to lie at about 250 KeV. At this energy the Compton and photoelectric cross-sections are equal. At the highest energy used here, 2.62 MeV, the contribution of multiple interactions is dominant. As an example, if the full energy peak at this energy were produced exclusively by three-fold events regarded as random samples, (e.g. pair plus the capture of both annihilation quanta) the transfer variance would be reduced to about 40% of the value for the crystal as a whole. Although the situation is actually a good deal more complex than this simple illustration, this is of about the magnitude of the observed fall in transfer variance between 250 KeV and 2.62 MeV. While it is doubtful whether any real physical meaning can be attached to an extrapolation of the transfer variance curve to even higher energies because of the increasing importance of edge and escape effects, it is nevertheless worthwhile to remark that even if these latter could

be eliminated, the curve would still not extrapolate to zero at infinite energy. Only if every event produced light uniformly throughout the volume of the crystal would this occur, and the discrete character of the processes by which gamma-rays convert their energy to light precludes this possibility.

Bisi and Zappa (1958) have also analysed the dependence of line-width on energy. In a statistical sense their argument is formally identical with that presented here. However, the data on intrinsic resolution were not abailable to them and their method of analysis implies that the transfer variance for a single interaction is independent of energy. While this may very well be true for very low gamma-ray energies, it does not seem likely that all energies as the survey in the liquid scintillator, discussed in Section 4.6 shows. Here considerable point-to-point variations were observed in a scintillator of the same geometric size on the same photomultiplier. Insofar as the variations observed paralleled closely the non-uniformity of the photo-cathode a similar variation may be expected within the sodium iodide crystal, although because of its different optical properties (e.g. surface finish, reflector), an exact quantitative correspondence is not to be expected. While it does not seem sensible to make detailed quantitative comparisons between the two scintillators, it is perhaps worthwhile to make a cautious semi-quantitative one. The transfer variance was measured in the liquid scintillator as $\eta^2 = 17 \times 10^{-4}$. If the frequency distribution of transfer probabilities were Gaussian, which is only approximately true, this would correspond

to a value for η^2 of about 90×10^{-4} which is rather larger than the data in Fig. 19 would lead us to expect. However, since this is an equally weighted average over the whole volume of the scintillator and makes no allowance for the unequal weights for primary events due to the exponential absorption in the scintillator, it certainly represents an extreme upper limit. A calculation based on primary events and allowing for absorption, reduces the above figure to about 60×10^{-4} at 663 KeV and this is consistant with the observations. The liquid scintillator survey also suggests the course of curve C at lower energies. Taking the transfer variance for the top 0.5 cm. of the crystal only, we obtain a value 4.7×10^{-4}, i.e., a contribution of 25×10^{-4} to η^2 from transfer effects at about 100 KeV and the curve C (Fig. 19) has therefore been extended to this value at 100 KeV to suggest the behaviour at lower energies. This argument also implies that the contribution from delta-rays continues to increase below 200 KeV. It should be emphasized again that the numerical values quoted here should not be taken too seriously since they are based on measurements in a different scintillator.

DISCUSSION:-

Thus this thesis presents a sufficiently coherent picture to suggest that a reasonably satisfactory set of statistical models has been found to describe the performance of the photomultiplier in a scintillation assembly. In particular, expression $f(x) = N^{\frac{1}{2}} a^{-\frac{1}{2}} e^{-n} x^{-\frac{1}{2}} \exp\left(\frac{-x}{\alpha}\right) I_1 \exp\left\{2(N x/a^{\frac{1}{2}})\right\}$ can probably be regarded as a sufficiently good representation of the shape of the ideal scintillation line even in cases where the simple exponential model from which it was derived is not applicable.

Expression (2), $V_G = (1 - V_m)(n\tau)^{-1}$, shows that so far as the photomultiplier is concerned, better resolution can be achieved by increasing the probability that a primary photon will result in an electron arriving at the 1st dynode, (which is well-known) or to a lesser extent and within limits, by decreasing V_m, the relative variance for multiplication process. The smallest value of V_m observed in the present work is already 0.63 for the 6810A, and it would appear that little improvement may be expected in this regard. For example, the smallest possible value of V_m for a distribution of the type (9.2) is in fact about 0.3 with ξ approximately ten.

It has already been remarked (Section 2.2) that the observed single-electron distributions are not consistant with a Poisson model for the statistics of dynode multiplication. The quasi-exponential character of these distributions invite comparison with proportional counters. Breitenberger has discussed the close formal analogy between

scintillation and proportional counters and points out that the only essential difference is that in a proportional counter the transfer efficiency is 100%. Snyder (1947), discussing proportional counters, shows that a simple duplication process leads to an exponential single-electron distribution and Frisch (quoted by Wilkinson (1950)) comes to a similar conclusion. The measurements of Curran et al (1948), show that the single-electron distribution can be represented by a relation of the type (9.3) with $\xi = 0.5$. It can also be fitted with a relation of type (9.2). These results suggest that the process of secondary emission in photomultipliers is much more closely represented by a duplication model in which the secondary electrons are more strongly correlated than the Poisson model often assumed, in which the individual secondary electrons must be assumed to be emitted independently of each other.

Comparison between non-crystalline organic scintillators such as NE 219 and a sodium iodide crystal of similar size suggests that for gamma-rays detection, an important contribution to line width originates with variations in the light collection efficiency from different regions of the scintillator.

References

1. Allen, J.S., 1950, Proc. I.R.E. 38, 346.

2. Baicker, J. A., 1960. I.R.E. Trans. Nuc. Sci. Ns-7, Nos. 3-4, 76.

3. Barnaby, C. F., and Barton, J. C., 1960. Proc. Phys. Soc. London, 76, 745.

4. Barlet, M. S., 1956. "Introduction to stochastic processes", Cambridge Univ. Press, p. 4 ff.

5. Bernstein, W., 1956. Nucleonics, 14, No. 4, 46.

6. Berger, M. J., and Doggett, J., 1956. Rev. Sci. Instr. 27, 269.

7. Bisi, A., and Zappa, L., 1958. Nuclear Instr. 3, 17.

8. Brietenberger, E., 1955. "Progress in nuclear physics", Vol. 4 ed. O.R. Frisch,Pergaman Press, London.

9. Brini, D., Peli L., Rimondi, O., and Veronesi, P., 1955. Nuovo Cim. Suppl., 2, 1048.

10. Burch, P. R. J., 1961. Proc. Phys. Soc. London, 77, 1125.

11. Campbell, G. A., and Foster, R. M., 1960. "Fourier Integrals for practical applications". Van Nostrand, New York.

12. Cramer, H., 1958. "Mathematical methods of statistics". Princeton Univ. Press.

13. Cummins, D.O., Delaney, C. F. G., and McAuly, I. R., 1960. Sci. Proc. Roy. Dyblin Soc., 1, 21.

14. Drapper, J. E., and Hickock, R. L., 1958. Rev. Sci. Instr. 29, 1047.

15. Erbacher, O., and Phillip, K., 1928. Zeit. fur physik. 51, 309.

16. Evans, R. D., 1955. "The atomic nucleus". McGraw-Hill, New York, page 663.

17. Garlick, C. J. F., and Wright, G. T., 1952. Proc. Phys. Soc. London, 65B, 415.

18. Hickock, R. L. and Drapper, J. E., 1958. Rev. Sci. Instr. 29, 994.

19. Iredale, P., 1961. Nucl. Instr. and Methods 21, 340.

20. Kelly, G. G., Bell., P. R., Davis, R. C., and Lazer, N. H., 1956. Nucleonics, 14, No. 4, 53.

21. Kikushkin, L. S., and Ratner, A. M., 1958. Zhur. Tekh. Fiz. 28, 345. translation: Soc. Phys. Tech. Phys 3, 318 (1958).

22. Lazar, N. H., Davis, R. C., and Bell., P. R., 1956. Nucleonics 14, No. 4, 52.

23. Lombard, F. J., and Martin, F., 1961. Rev. Sci. Instr. 32, 200.

24. Mahagan, W. W., 1962. I. R. E. Trans. Nuc. Sci. NS-9, No. 3, 1.

25. Morton, G. A., and Mitchell, J. A., 1949. Nucleonics 4, No. 1, 16.

26. Morton, G. A., and Mitchell, J. A., 1948. R.C.A. Review 9, 632.

27. Mott, W. E., and Sutton, R. B., 1958. "Scintillation and erenkov counter". Handbuch der physik, Vol. 45, Springerverlag, Berlin, p. 86.

28. Murray, R. B., and Meyer, A., 1961. Phys. Rev. 122, 815.

29. Nelms, A. T., 1953. N.B.S. Circular 542, Washington, D.C.

30. Prescott, J. R., and Takhar, P. S., 1962. I.R.E. Trans. Nuc. Sci. NS-9, No. 3, 36.

31. Prescott, J. R., and Lindquist, D. L., 1961. Rev. Sci. Instr. 32, 990.

32. Ratner, A. M., and Kukuskin, L. S., 1958. Zhur. Tekh. Fiz. 28, 1121. Translation: Soc. Phys. Tech. Phys. 3, 1044.

33. Roberts, P. W., 1953. Proc. Phys. Soc. London, A66, 192.

34. Swank , R. K., Buck, W. L., 1952. Nucleonics 10, No. 5, 51.

35. Wright, G. T., 1954. J. Sci. Instr. 31, 337 and 462.

36. Wright, G. T., and Garlick, G. F. J., 1954. Brit. J. Appl. Phys. 5, 13.

37. Zerby, C. D., Meyer, A., and Murray, R. B., 1961. Nuclear Instr. and Methods 12, 115.

APPENDIX I

Derivation of generating functions for Poisson, Binomial and exponential distributions:

(i) The poisson distribution is given by

$$p(x) = \frac{e^{-n} n^x}{x!}$$

where x = 0,1,2 .....

The generating function by definition is given

$$M(\theta) = \sum_{x=0}^{\infty} \theta^x e^{-n} \frac{n^x}{x!}$$

$$= e^{-n} \sum_{x=0}^{\infty} \frac{(\theta n)^x}{x!}$$

$$= e^{-n} e^{n\theta}$$

$$\therefore \quad M(\theta) = e^{n(\theta-1)}$$

which is the generating function for Poisson distribution.

(ii) The binomial distribution is given by

$$T(x) = \binom{n}{x} r^x q^{n-x}$$

$$M(\theta) = \sum_{x=0}^{\infty} \theta^x \binom{n}{x} r^x q^{n-x} \quad \text{where } x = 0,1,2 \ldots n.$$

$$= \sum_{x=0}^{\infty} \binom{n}{x} (r\theta)^x q^{n-x}$$

$$= (q + r\theta)^n$$

$$= \left[(1-r) + r\theta\right]^n$$

which is generating function for binomial distribution.

$$f(x) = \frac{1}{\alpha} e^{-\alpha x} \qquad 0 \leq x < \infty$$

(iii) The exponential distribution was of the form

$$f(x) = \frac{1}{\alpha} e^{-\alpha x} \qquad 0 \leq x < \infty$$

and the generating function is:

$$M(\theta) = \int_0^\infty \theta^x \frac{1}{\alpha} e^{-\frac{x}{\alpha}} \, dx = \frac{1}{\alpha} \int_0^\infty e^x \left(\log\theta - \frac{1}{\alpha} \right) dx$$

$$= \frac{1}{\alpha \log\theta - 1} \left[e^{x\left(\log\theta - \frac{1}{\alpha}\right)} - 1 \right]_0^\infty$$

$$\therefore \quad M(\theta) = \frac{1}{1 - \alpha \log\theta} \qquad \frac{1}{\alpha} > \log\theta$$

APPENDIX II

Finding the mean = Na and Variance = $2Na^2$

We have three generating functions for poisson, binomial and exponential distributions, i.e.

$$G_1 = \exp(n(\theta - 1))$$

$$G_2 = [r\theta - (1-r)] \qquad n = 1$$

$$G_3 = \frac{1}{1 - a\log\theta}$$

The generating function for all the three processes combined is given by:

$$G(z) = G_1(G_2(G_3(\theta)))$$

$$= \exp\left\{ n\left[\frac{r}{1 - a\log\theta} + (1-r) - 1 \right] \right\}$$

$$= \exp\left\{ n\left(\frac{r - r + ar\log\theta}{1 - a\log\theta} \right) \right\}$$

$$G(z) = \exp\left\{ \frac{nar\log\theta}{1 - a\log\theta} \right\}$$

For the characteristic function $\log\theta$ is replaced by $i\theta$ and we have the characteristic function:

$$f(\theta) = \exp\left\{ \frac{anri\theta}{1 - ia\theta} \right\} = \exp\left\{ \frac{ianr\theta}{1 - ia\theta} \right\}$$

$N = nr$

$$= \exp\left\{ \frac{N}{1 - ia\theta} - N \right\}$$

Writing $\quad f(\theta) = M(\theta) = \exp\left\{ \frac{N}{1 - ia\theta} - N \right\}$

$$\therefore \quad M'(\theta) = \exp\left\{ \frac{N}{1 - ia\theta} - N \right\} \frac{N}{(1 - ia\theta)^2} ia$$

When $\theta = 0$, the first moment or mean is

$$\mu_1' = M'(0) = Na$$

Hence the mean is

$$\mu_1' = Na$$

Hence the mean is

$$\mu_1' = Na.$$

For finding the second moment write:

$$\frac{Nia}{(1-ia\theta)^2} = N(\theta)$$

then

$$M''(\theta) = M(\theta)\, N(\theta)' + N(\theta)\, M(\theta)'$$

$$= M(\theta)\, \frac{2Na^2}{(1-ia\theta)^3} + \frac{Na}{(1-ia\theta)^2}\, M(\theta)\, \frac{N.a}{(1-ia\theta)^2}$$

$$= M(\theta) \left[\frac{2Na^2 + N^2a^2}{(1-ia\theta)^3} \right]$$

The second moment is

$$\mu_2' = M''(0) = 2Na^2 + N^2a^2$$

Hence the variance is

$$\sigma^2 = \mu_2 = \mu_2' - \mu_1^2$$

$$= 2Na^2 + N^2a^2 - N^2a^2$$

$$\therefore \quad \sigma^2 = 2Na^2$$

Derivation of the relation $VG = 1 + Vm/mr$

If μ_x, μ_y, μ_z represent the means of the frequency functions f_x, f_y, f_z respectively, then the mean is

$$\mu_G = \mu_x \mu_y \mu_z.$$

Introducing the dimensionless relative variance

$$V = \frac{\text{variance}}{(\text{mean})^2}$$

$$= \frac{\sigma^2}{\mu^2}$$

then

$$V_G = V_x + \frac{V_y}{\mu_x} + \frac{V_z}{\mu_x \mu_y}$$

Further making no assumption about the model to be used for dynode statistics, then on the basis of three-stage chain consisting of Poisson light production, binomial transfer and multiplication or arbitrary, model, with relative variance Vm, the relation (1) (of Chapter 2) is taken in the form of

$$V_G = V_m + \frac{r(1-r)}{r^2 m} + \frac{V_m}{mr}$$

where r is mean, $r(1-r)$ is the variance for the binomial distribution.

Simplifying,

$$V_G = \left(V_m - \frac{1}{m}\right) + \frac{1 + V_m}{mr}$$

If the luminous mechanism is such that

$$V_m = \frac{1}{m}$$

then above reduces to

$$V_G = \frac{1 + V_m}{mr}$$